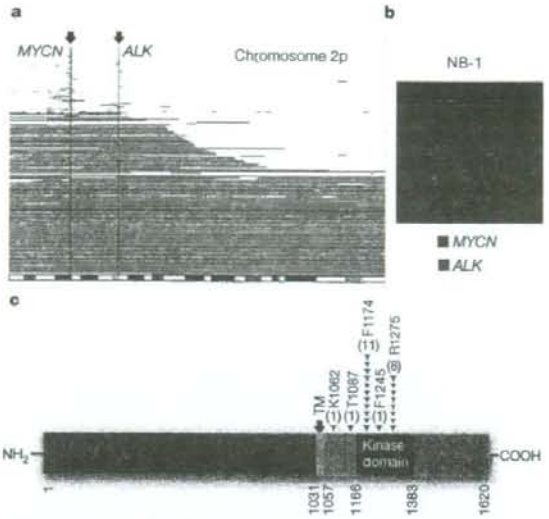

Figure 1 | Common 2p gains/amplifications and *ALK* mutations in neuroblastoma samples. a, Recurrent copy number gains on the 2p arm. High-grade amplifications are shown by light-red horizontal lines, whereas simple gains are shown by dark-red lines. Two common peaks of copy number gains and amplifications in the *MYCN* and *ALK* loci are indicated by arrows. The cytobands in 2p are shown at the bottom. **b**, Interphase FISH analysis of NB-1 showing high-grade amplification of *MYCN* (red) and *ALK* loci (green). The amplified *MYCN* locus appears as a single large signal. **c**, Distribution of the eight *ALK* mutations found in 21 neuroblastoma samples. The positions of the mutated amino acids are indicated by black (primary samples) and red (cell lines) arrowheads. The number of mutations at each site is shown at the top of the arrowheads. TM, transmembrane.

(6.1%) primary samples and 8 out of 24 (33%) cell lines, which resulted in seven types of amino acid substitutions at five different positions (Table 1 and Supplementary Fig. 6). They were not found in either the genomic DNA collected from 50 healthy volunteers or in the SNP databases at the time of preparing this manuscript. In fact, somatic origins of missense changes were confirmed in 9 out of 13 primary cases, for which DNA was obtained from the peripheral blood or the tumour-free bone marrow specimens (Supplementary Fig. 6). On the other hand, T1087I (ACC>ATC), found in case NT126, had a germline origin and thus it could not be determined whether the T1087I change was a rare non-functional polymorphism or represented a pathogenic germline mutation. For other changes found in three primary cases (NT128, NT217 and NT218) and cell lines, normal DNA was not available but they were likely to represent oncogenic mutations because they were identical to common somatic changes (F1174L or R1275Q) or shown to have oncogenic potential in functional assays (K1062M).

Most mutations occurred within the kinase domain (20 out of 22 or 91%), which clearly showed two mutation hotspots at F1174 and R1275 (Fig. 1c). A neuroblastoma-derived cell line, SJNB-2, had a homozygous *ALK* mutation of R1275Q, which was probably due to uniparental disomy of chromosome 2 (Supplementary Fig. 7a). Another case (NT074) harboured two different mutations, F1174L and R1275Q, but it remains to be determined whether both are on the same allele. ALK mutations within the kinase domain occurred at amino acid positions that are highly conserved across species and during molecular evolution (Supplementary Figs 8 and 9). According to the conserved structure of other insulin receptor kinases we predicted that F1174 is located at the end of the Cα1 helix, whereas the other two are on the two β-sheets: before the catalytic loop (β6, F1245) and within the activation loop (β9, R1275) (Supplementary Fig. 7b, c)[17]. Thus, conformational changes due to amino acid substitutions at these positions might be responsible for the aberrant activity of the mutant kinases.

Table 1 | *ALK* mutations/amplifications in neuroblastoma samples

Sample	Age (months)	Stage	*MYCN**	Clinical outcome	Mutations/ amplifications	Nucleotide substitution	Origin of mutations
NT126	99	4	−	Dead	T1087I	ACC>ATC	Germ line
NT218	8	1	−	Alive	F1174L	TTC>TTG	ND
NT074	34	3	+	Dead	F1174L	TTC>TTA	Somatic
					R1275Q	CGA>CAA	
NT160	12	4	+	Dead	F1174L	TTC>TTA	Somatic
NT217	24	4	+	Dead	F1174L	TTC>TTA	ND
NT190	48	4	+	Alive	F1174L	TTC>TTA	Somatic
NT060	163	3	−	Alive	F1174C	TTC>TGC	Somatic
NT162	28	4	+	Dead	F1174V	TTC>GTC	Somatic
NT195	24	4	+	Alive	F1245L	TTC>TTG	Somatic
NT055	6	3	−	Alive	R1275Q	CGA>CAA	Somatic
NT128	8	4	−	Dead	R1275Q	CGA>CAA	ND
NT164	54	4	+	Dead	R1275Q	CGA>CAA	Somatic
NT200	133	4	−	Dead	R1275Q	CGA>CAA	Somatic
SCMC-N5†	-	-	+	-	K1062M	AAG>ATG	ND
SJNB-4†	-	-	+	-	F1174L	TTC>TTA	ND
LAN-1†	-	-	+	-	F1174L	TTC>TTA	ND
SCMC-N2†	-	-	+	-	F1174L	TTC>TTA	ND
SK-N-SH†	-	-	−	-	F1174L	TTC>TTA	ND
SJNB-2†‡	-	-	+	-	R1275Q	CGA>CAA	ND
LAN-5†	-	-	+	-	R1275Q	CGA>CAA	ND
TGW†	-	-	+	-	R1275Q	CGA>CAA	ND
NT204	12	1	+	Alive	Amplification	-	-
NT056	11	3	−	Dead	Amplification	-	-
NT071	36	3	+	Alive	Amplification	-	-
NT165	19	4	+	Dead	Amplification	-	-
NT169	7	4	+	Dead	Amplification	-	-
NB-1†	-	-	+	-	Amplification	-	-

ND, not determined.
* Presence (+) or absence (−) of *MYCN* amplification in FISH analysis. All cases where there was an absence of *MYCN* amplification (−) were also checked for possible *MYCN* mutations by sequencing of all *MYCN* exons, but no *MYCN* mutations were identified.
† Cell lines.
‡ Homozygous mutation.

ALK mutation highly correlated with *MYCN* amplification ($P = 1.55 \times 10^{-4}$, Fisher's exact test; Supplementary Table 6) where 14 out of 21 mutations coexisted with *MYCN* amplification. Regardless of the status of *MYCN* amplification, 12 of the 13 mutations were found in patients with advanced stage neuroblastoma (Table 1). However, whereas *MYCN* amplification and stage 4 were significant risk factors for poor survival, the mutation/amplification status of *ALK* was not likely to have a major impact on survival (Supplementary Fig. 10 and Supplementary Table 7), although the statistical power of the current analysis was largely limited in order to detect a marginal hazard.

To evaluate the impact of ALK mutations on kinase activity, we generated Flag-tagged constructs of ALK and its mutants, F1174L and K1062M, which were stably expressed in NIH3T3 cells, and examined their phosphorylation status and *in vitro* kinase activity. The ALK mutants stably expressed in NIH3T3 cells were phosphorylated according to western blot analysis using an antibody specific for phosphorylated ALK (anti-pY1604) and a PY20 blot after anti-Flag immunoprecipitation of the mutant kinases (Fig. 2a), whereas the wild-type kinase was not phosphorylated. The immunoprecipitated ALK mutants also showed increased tyrosine kinase activity *in vitro* when compared with wild-type ALK. This was shown using both a universal substrate for tyrosine kinase (poly-GluTyr) and the synthetic YFF peptide[18], which was derived from a sequence of the activation loop of *ALK* (Fig. 2b, c). In accordance with these findings, downstream molecules of ALK signalling including AKT, STAT3 and ERK[15] were activated in cells expressing mutant ALK, as shown by their increased phosphorylation (Fig. 2d).

Next, we investigated the oncogenic potential of these mutants. NIH3T3 cells stably expressing mutant kinases showed increased colony formation in soft agar compared with the wild-type protein (Fig. 3a and Supplementary Fig. 11). The tumorigenicity of these ALK mutants was further assayed by injecting 1.0×10^7 NIH3T3 cells into nude mice. The NIH3T3 cells transfected with the ALK mutants showed focus-forming capacity and developed subcutaneous tumours (6 out of 6 inoculations) 21 days after inoculation, whereas the mock and wild-type ALK-transfected cells did not (0 out of 6 inoculations) (Fig. 3b, c). Finally, we examined the effect of ALK inhibition on the proliferation of neuroblastoma-derived cell lines. RNA interference (RNAi)-mediated *ALK* knockdown resulted in reduced cell proliferation of SK-N-SH cells harbouring the F1174L mutation, but the effects were less clear in wild-type ALK-expressing LAN-2 cells (Fig. 3d, e). Of particular interest is a recent report that 5 out of 17 neuroblastoma-derived cell lines, including SK-N-SH and NB-1, frequently showed high sensitivity to the specific ALK inhibitor TAE684 (ref. 19).

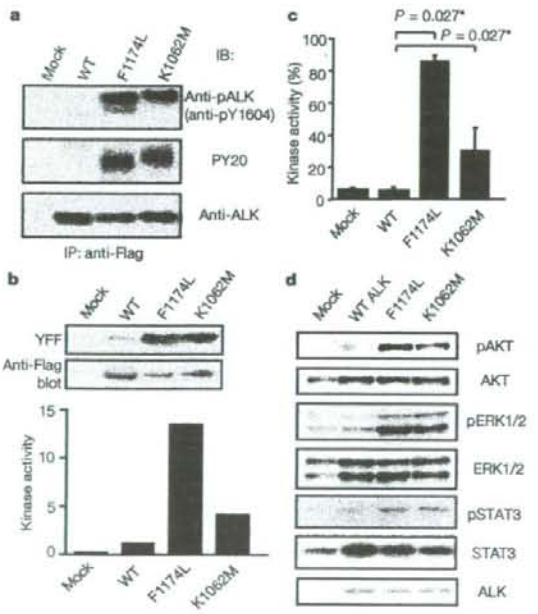

Figure 2 | Kinase activity of ALK mutants and their downstream signalling. **a**, Stably expressed ALK and its mutants (F1174L and K1062M) were immunoprecipitated with an anti-Flag antibody and subjected to western blot analysis with anti-pY1604 (upper panel) or PY20 (middle panel). An anti-ALK blot of precipitated kinases is also displayed (bottom panel). **b**, *In vitro* kinase assay for wild-type ALK kinase and its mutants using the synthetic YFF peptide as a substrate, where kinase activity is expressed as relative values to that for wild-type kinase based on the densities in the autoradiogram. **c**, Kinase activity was also assayed for the poly-GluTyr peptide. Significantly different measurements are indicated by asterisks with *P* values. Bars show mean (±s.d.) in three independent experiments. **d**, Western blot analyses of NIH3T3 cells expressing wild-type and mutant ALK for phosphorylated forms of AKT (pAKT), ERK (pERK1/2) and STAT3 (pSTAT3). The total amount of each molecule is also displayed (AKT, ERK1/2, and STAT3) together with an anti-ALK blot (ALK).

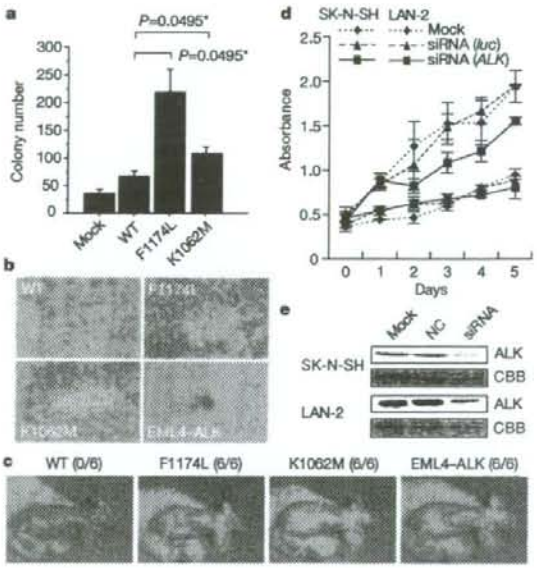

Figure 3 | Oncogenic role of ALK mutations. **a**, Colony assays for NIH3T3 cells stably expressing wild-type as well as mutant ALK (F1174L and K1062M). The average numbers of colonies in triplicate experiments are plotted and standard deviation is indicated. Results showing statistically significant differences as compared with experiments using wild-type ALK are indicated by asterisks with *P* values. **b**, **c**, NIH3T3 cells were transfected with wild-type and mutant ALK (F1174L, K1062M and EML4–ALK) and subjected to a focus forming assay (**b**) as well as an *in vivo* tumorigenicity assay in nude mice (**c**). **d**, Effect of RNAi-mediated ALK knockdown on cell proliferation in neuroblastoma cell lines expressing either the F1174L mutant (SK-N-SH) or wild-type ALK (LAN-2). Cell growth was measured using the Cell Counting Kit-8 after knockdown experiments using *ALK*-specific siRNAs (siRNA *ALK*), control siRNAs (siRNA *luc*), or mock experiments, where absorbance was measured in triplicate and averaged for each assay. To draw growth curves, the mean ± s.d. of the averaged absorbance in three independent knockdown experiments is plotted. **e**, Successful knockdown of ALK protein was confirmed by anti-ALK blots (ALK) using Coomassie brilliant blue G-250 (CBB) staining as loading controls. NC, control siRNA; siRNA, *ALK* siRNA.

Through the genome-wide analysis of genetic lesions in neuroblastoma, we identified novel oncogenic *ALK* mutations in advanced neuroblastoma. Combined with the cases having a high-grade amplification of the *ALK* gene, aberrant ALK signalling was likely to be involved in 11% (16 out of 151) of the advanced neuroblastoma cases. Because ALK kinase has been shown to be deregulated only in the form of a fusion kinase in human cancers, including lymphoma and lung cancer, the identification of oncogenic mutations in *ALK* not only increases our understanding of the molecular pathogenesis of advanced neuroblastoma, but also adds a new paradigm to the concept of 'ALK-positive human cancers' in that the mutated *ALK* kinases themselves might participate in human cancers. Our results again highlight the power of genome-wide studies to clarify the genetic lesions in human cancers[20–22]. Given that *ALK* mutations are preferentially involved in advanced neuroblastoma cases having a poor prognosis, our findings implicate that *ALK* inhibitors may improve the clinical outcome of children suffering from intractable neuroblastoma.

METHODS SUMMARY

Genomic DNA from 215 patients with primary neuroblastoma and 24 neuroblastoma-derived cell lines was analysed on GeneChip SNP genotyping microarrays (Affymetrix GeneChip 250K *Nsp*I). After appropriate normalization of mean array intensities, signal ratios were calculated between tumours and anonymous normal references in an allele-specific manner, and allele-specific copy numbers were inferred from the observed signal ratios based on the hidden Markov model using CNAG/AsCNAR software[13,14]. *ALK* mutations were examined by DNA heteroduplex analysis and/or genomic DNA sequencing[16]. Full-length cDNAs for mutant *ALK* were isolated by high-fidelity PCR and inserted into pcDNA3 and pMXS. The expression plasmids were transfected into NIH3T3 cells using Effectene Transfection Reagent (Qiagen) or by calcium phosphate methods[9]. Western blot analysis of mutant ALK kinases, *in vitro* kinase assays, and tumour formation assays in nude mice were performed as previously described[9]. This study was approved by the ethics boards of the University of Tokyo and of the Chiba Cancer Center Research Institute.

Full Methods and any associated references are available in the online version of the paper at www.nature.com/nature.

Received 3 June; accepted 28 August 2008.

1. Maris, J. M., Hogarty, M. D., Bagatell, R. & Cohn, S. L. Neuroblastoma. *Lancet* 369, 2106–2120 (2007).
2. Maris, J. M. *et al.* Loss of heterozygosity at 1p36 independently predicts for disease progression but not decreased overall survival probability in neuroblastoma patients: a Children's Cancer Group study. *J. Clin. Oncol.* 18, 1888–1899 (2000).
3. Attiyeh, E. F. *et al.* Chromosome 1p and 11q deletions and outcome in neuroblastoma. *N. Engl. J. Med.* 353, 2243–2253 (2005).
4. Bown, N. *et al.* Gain of chromosome arm 17q and adverse outcome in patients with neuroblastoma. *N. Engl. J. Med.* 340, 1954–1961 (1999).
5. Brodeur, G. M., Seeger, R. C., Schwab, M., Varmus, H. E. & Bishop, J. M. Amplification of N-myc in untreated human neuroblastomas correlates with advanced disease stage. *Science* 224, 1121–1124 (1984).
6. Shiota, M. *et al.* Anaplastic large cell lymphomas expressing the novel chimeric protein p80NPM/ALK: a distinct clinicopathologic entity. *Blood* 86, 1954–1960 (1995).
7. Morris, S. W. *et al.* Fusion of a kinase gene, ALK, to a nucleolar protein gene, NPM, in non-Hodgkin's lymphoma. *Science* 263, 1281–1284 (1994).
8. Fujimoto, J. *et al.* Characterization of the transforming activity of p80, a hyperphosphorylated protein in a Ki-1 lymphoma cell line with chromosomal translocation t(2;5). *Proc. Natl Acad. Sci. USA* 93, 4181–4186 (1996).
9. Soda, M. *et al.* Identification of the transforming *EML4–ALK* fusion gene in non-small-cell lung cancer. *Nature* 448, 561–566 (2007).
10. Rikova, K. *et al.* Global survey of phosphotyrosine signaling identifies oncogenic kinases in lung cancer. *Cell* 131, 1190–1203 (2007).
11. Kennedy, G. C. *et al.* Large-scale genotyping of complex DNA. *Nature Biotechnol.* 21, 1233–1237 (2003).
12. Matsuzaki, H. *et al.* Genotyping over 100,000 SNPs on a pair of oligonucleotide arrays. *Nature Methods* 1, 109–111 (2004).
13. Nannya, Y. *et al.* A robust algorithm for copy number detection using high-density oligonucleotide single nucleotide polymorphism genotyping arrays. *Cancer Res.* 65, 6071–6079 (2005).
14. Yamamoto, G. *et al.* Highly sensitive method for genomewide detection of allelic composition in nonpaired, primary tumor specimens by use of affymetrix single-nucleotide-polymorphism genotyping microarrays. *Am. J. Hum. Genet.* 81, 114–126 (2007).
15. Osajima-Hakomori, Y. *et al.* Biological role of anaplastic lymphoma kinase in neuroblastoma. *Am. J. Pathol.* 167, 213–222 (2005).
16. Donohoe, E. Denaturing high-performance liquid chromatography using the WAVE DNA fragment analysis system. *Methods Mol. Med.* 108, 173–187 (2005).
17. Hu, J., Liu, J., Ghirlando, R., Saltiel, A. R. & Hubbard, S. R. Structural basis for recruitment of the adaptor protein APS to the activated insulin receptor. *Mol. Cell* 12, 1379–1389 (2003).
18. Donella-Deana, A. *et al.* Unique substrate specificity of anaplastic lymphoma kinase (ALK): development of phosphoacceptor peptides for the assay of ALK activity. *Biochemistry* 44, 8533–8542 (2005).
19. McDermott, U. *et al.* Genomic alterations of anaplastic lymphoma kinase may sensitize tumors to anaplastic lymphoma kinase inhibitors. *Cancer Res.* 68, 3389–3395 (2008).
20. Garraway, L. A. *et al.* Integrative genomic analyses identify MITF as a lineage survival oncogene amplified in malignant melanoma. *Nature* 436, 117–122 (2005).
21. Mullighan, C. G. *et al.* Genome-wide analysis of genetic alterations in acute lymphoblastic leukaemia. *Nature* 446, 758–764 (2007).
22. Kawamata, N. *et al.* Molecular allelokaryotyping of pediatric acute lymphoblastic leukemias by high-resolution single nucleotide polymorphism oligonucleotide genomic microarray. *Blood* 111, 776–784 (2008).

Supplementary Information is linked to the online version of the paper at www.nature.com/nature.

Acknowledgements We thank H. P. Koeffler for critically reading and editing the manuscript. We also thank M. Matsumura, Y. Ogino, S. Ichimura, S. Sohma, E. Matsui, Y. Yin, N. Hoshino and Y. Nakamura for their technical assistance. This work was supported by the Core Research for Evolutional Science and Technology, Japan Science and Technology Agency and by a Grant-in-Aid from the Ministry of Health, Labor and Welfare of Japan for the third-term Comprehensive 10-year Strategy for Cancer Control.

Author Contributions Y.C., Y.L.C. and J.T. contributed equally to this work. M.K. and M.Sa. performed microarray experiments and subsequent data analyses. Y.C. and J.T. performed mutation analysis of *ALK*. Y.C., Y.L.C., J.T., M.So., L.W. and H.M. conducted functional assays of mutant ALK. A.N., M.O., T.I., A.K. and Y.H. prepared tumour specimens and were involved in statistical analysis. A.N., Y.H., H.M., J.T. and S.O. designed the overall study, and S.O. and J.T. wrote the manuscript. All authors discussed the results and commented on the manuscript.

Author Information The nucleotide sequences of *ALK* mutations detected in this study have been deposited in GenBank under the accession numbers EU788003 (K1062M), EU788004 (T1087I), EU788005 (F1174L; TTC/TTA), EU788006 (F1174L; TTC/TTG), EU788007 (F1174C), EU788008 (F1174V), EU788009 (F1245L) and EU788010 (R1275Q). The copy number data as well as the raw microarray data will be accessible from http://www.ncbi.nlm.nih.gov/geo/ with the accession number GSE12494. Reprints and permissions information is available at www.nature.com/reprints. Correspondence and requests for materials should be addressed to S.O. (sogawa-tky@umin.net) or Y.H. (hayashiy-tky@umin.ac.jp).

METHODS

Specimens. Primary neuroblastoma specimens were obtained during surgery or biopsy from patients who were diagnosed with neuroblastoma and admitted to a number of hospitals in Japan. In total, 215 primary neuroblastoma specimens were subjected to SNP array analysis after informed consent was obtained from the parents of each patient. The patients were staged according to the International Neuroblastoma Staging System[23]. The clinicopathological findings are summarized in Supplementary Table 1. Twenty-four neuroblastoma-derived cell lines were also analysed by SNP array analysis (Supplementary Table 2). The SCMC-N2, SCMC-N4 and SCMC-N5 cell lines were established in our laboratory[24,25]. The SJNB series of cells and the UTP-N-1[26] cell line were gifts from A. T. Look and A. Inoue, respectively. The other cell lines used were obtained from the Japanese Cancer Resource Cell Bank (http://cellbank.nibio.go.jp/).

Microarray analysis. High molecular mass DNA was isolated from tumour specimens as well as from the peripheral blood or the bone marrow as described previously[24]. The DNA was subjected to SNP array analysis using Affymetrix GeneChip Mapping 50K and/or 250K arrays (Affymetrix) according to the manufacturer's suggested protocol. The scanned array images were processed with Gene Chip Operation software (GCOS)[13], followed by SNP calls using GTYE. Genome-wide copy number measurements and loss of heterozygosity detection were performed using CNAG/AsCNAR algorithms[14], which enabled an accurate determination of allele-specific copy numbers.

Confirmation of SNP array data. FISH and/or genomic PCR analysis confirmed the results of SNP array analyses as described previously[15]. PCR primer sets were designed to amplify several adjacent fragments inside and outside of the homozygously deleted regions in tumour samples.

Mutation analysis. Mutations in the *ALK* gene were examined in 239 neuroblastoma samples, including 24 cell lines, by denaturing high-performance liquid chromatography (DHPLC) using the WAVE system (Model 4500; Transgenomic) according to the manufacturer's suggested protocol[16]. The samples showing abnormal conformations were subjected to direct sequencing analysis using an ABI PRISM 3100 Genetic Analyser (Applied Biosystems). Using direct sequencing, mutation analysis of *MYCN* was also performed in seven cases with *ALK* alterations but not *MYCN* amplification. The primer sets used in this study are listed in Supplementary Table 5.

Transforming potential of *ALK* mutants. Total RNA was extracted from SJNB-1 (wild type), SCMC-N2 (F1174L) and SCMC-N5 (K1062M) cells as described previously[26]. First-strand cDNA was synthesized from RNA using Transcriptor Reverse Transcriptase and an oligo (dT) primer (Roche Applied Science). The resulting cDNA was then amplified by PCR using the KOD-Plus-Ver.2 DNA polymerase (Toyobo) and the primers sense 5′-TCAGAAGCTTTACCAAGGACTGTTCAGAGC-3′ and antisense 5′-AATTGCGGCCGCTACTTGTCATCGTCGTCCTTGTAGTCGGGCCCAGGCTG GTTCATGC-3′, thereby introducing a HindIII site at the 5′ terminus and a NotI site and a Flag sequence at the 3′ terminus. The HindIII–NotI fragments of *ALK* cDNA were subcloned into pcDNA3 to generate expression plasmids. After resequencing to confirm that they had no other mutations, the *ALK* plasmids were used for transfection into NIH3T3 cells using Effectene Transfection Reagent (Qiagen) according to the suggested manufacturer's protocol. The transfected NIH3T3 cells were selected in 800 $\mu g\,ml^{-1}$ G418 for 2 weeks to obtain stably expressing clones.

To evaluate the phosphorylation status of ALK mutants, the cell lysates of stable clones were immunoprecipitated with antibodies to Flag (Sigma) and the resulting precipitates were subjected to western blot analysis with the antibody specific to pTyr 1604 (Cell Signaling Technology) of ALK and the generic anti-phosphotyrosine antibody (PY20). The *in vitro* kinase activity of ALK mutants was measured using a non-radioactive isotope solid-phase enzyme-linked immunosorbent assay using the Universal Tyrosine Kinase Assay kit (Takara) according to the manufacturer's suggested protocol. We also performed the *in vitro* kinase assay with the synthetic YFF peptide (Operon Biotechnologies) as described previously[18]. For anchorage-independent growth analysis, 1×10^3 stably transfected NIH3T3 cells were mixed in 0.3% agarose with 10% FBS-DMEM and plated on 0.6% agarose-coated 35-mm dishes. After culture for 28 days, the colonies of >0.1 mm in diameter were counted. The quantification of the colonies was from three independent experiments. To investigate the downstream signalling of ALK, western blot analysis was performed using the anti-ERK1/2, anti-phospho-ERK1/2, anti-AKT, anti-phospho-AKT, anti-STAT3 and anti-phospho-STAT3 antibodies (Cell Signaling Technology)[18].

The cDNA mutant of *ALK* was also inserted into the pMXS plasmid and the constructs were introduced into NIH3T3 cells by the calcium phosphate method as described previously[8]. The cells were then either cultured for 21 days or injected subcutaneously at six sites in three nude mice.

Inhibition of ALK through RNAi-mediated knockdown. To suppress the expression of the ALK protein, two different pairs of *ALK* siRNAs (*ALK* siRNA1 and *ALK* siRNA2) were obtained (Qiagen)[15]. The sequences were 5′-GAGUCUGGCAGUUGACUUCdTdT-3′ for *ALK* siRNA1 and 5′-GCUCCGGCGUGCCAAGCAGdTdT-3′ for *ALK* siRNA2. A siRNA, targeting a sequence in firefly (*Photinus pyralis*) luciferase mRNA (*luc* siRNA), was used as a negative control (Qiagen)[15]. The sequences of *luc* siRNA were as follow: sense 5′-CGUACGCGGAAUACUUCGAdTdT-3′ and antisense 5′-UCGAAGUAUUCCGCGUACGdTdT-3′. Gene knockdown was achieved in SK-N-SH and LAN-2 cells using HiPerFect transfection reagent following the manufacturer's suggested instructions (Qiagen). To assess the effect of ALK knockdown on cell growth, these cells were seeded in 96-well plates at a concentration of 8.0×10^3 cells per well 24 h before transfection and assayed using the Cell Counting Kit-8 (Wako).

Statistical analysis. The significance of the correlation between *MYCN* amplification and *ALK* mutation was tested according to the conventional 2×2 contingency table using Fisher's exact test. The significance of the differences in kinase activity between wild-type and mutant ALK kinases was examined by the Mann–Whitney *U*-test based on the measured percentage activity of kinases in the precipitates of the corresponding samples. The significance of the differences in colony formation between wild-type and mutant ALK kinases was also examined by the Mann–Whitney *U*-test. The size of the hazards from possible risk factors, including International Neuroblastoma Staging System stages, *MYCN* status and *ALK* mutation/amplification were estimated by Cox regression analysis assuming a proportional hazard model using Stata software. Correlation between ploidy and clinical stage was tested by nptrend test.

23. Smith, E. I., Haase, G. M., Seeger, R. C. & Brodeur, G. M. A surgical perspective on the current staging in neuroblastoma—the International Neuroblastoma Staging System proposal. *J. Pediatr. Surg.* 24, 386–390 (1989).
24. Takita, J. *et al.* Allelotype of neuroblastoma. *Oncogene* 11, 1829–1834 (1995).
25. Takita, J. *et al.* Absent or reduced expression of the caspase 8 gene occurs frequently in neuroblastoma, but not commonly in Ewing sarcoma or rhabdomyosarcoma. *Med. Pediatr. Oncol.* 35, 541–543 (2000).
26. Takita, J. *et al.* Allelic imbalance on chromosome 2q and alterations of the caspase 8 gene in neuroblastoma. *Oncogene* 20, 4424–4432 (2001).

Novel gain-of-function mutation in the extracellular domain of the *PDGFRA* gene in infant acute lymphoblastic leukemia with t(4;11)(q21;q23)

Leukemia (2008) **22**, 2279–2280; doi:10.1038/leu.2008.140; published online 12 June 2008

Platelet-derived growth factor receptors α and β (PDGFRA and PDGFRB) belong to the class III receptor tyrosine kinases, which include c-KIT, colony stimulating factor-1 receptor and FLT3.[1] *PDGFRA* and *c-KIT* are two related receptor tyrosine kinases showing similar structure, and mutations of these genes are detected in gastrointestinal stromal tumor[2,3] and myeloproliferative disorders.[4] Recently, we reported a *PDGFRA* N870S mutation in a 13-year-old boy having acute myelogenous leukemia (AML)-M1 with t(8;21) and an F808L mutation in a 13-year-old girl having AML-M1 with inv(16).[5] In addition to point mutations, the *FIP1L1-PDGFRA* fusion tyrosine kinase resulting from internal deletion of 4q12 locus was described in a subgroup of patients presenting hypereosinophilic syndrome.[6] Here, we investigated whether *PDGFRA* is also implicated in the pathogenesis of acute lymphoblastic leukemia (ALL), and found a mutation which renders a factor-dependent cell line factor-independent by its aberrant tyrosine phosphorylation.

One hundred and twenty seven childhood ALL and 40 infant ALL samples, including those from 13 patients with t(4;11)(q21;q23) (one patient was childhood ALL and the others were infant ALL), were analyzed for the expression and mutation of *PDGFRA*. *PDGFRA* gene was expressed in 38 (29.9%) of the 127 childhood ALL patient samples, 12 (30.0%) of the 40 infant ALL patients and 9 (36.0%) of the 25 ALL patients associated with *MLL* gene rearrangements. Sequence analyses of the samples expressing *PDGFRA* revealed a *PDGFRA* A509D mutation (Figure 1a) in a 4-month-old boy having ALL with t(4;11)(q21;q23). This mutation in the Ig5 domain of *PDGFRA* corresponds to those responsible for ligand-independent kinase activation of *c-KIT* in gastrointestinal stromal tumor.[3] Mutations on exon 9 encoding the extracellular domain near the transmembrane domain of *c-KIT* lead to ligand-independent activation of c-KIT,[2,3] and are associated with core binding factor AML and gastrointestinal stromal tumor.[1,3,7] We examined whether the mutation at Ig5 domain of the *PDGFRA* gene resulted in constitutive activation of the kinase activity by retroviral transduction[8] of the wild-type and mutated *PDGFRA* cDNAs into an IL-3 dependent mouse cell line, Ba/F3 and stable cell lines expressing each transgene were established. The whole coding region of *PDGFRA* cDNA was sequenced directly or after subcloning into a retroviral vector pMXs-IN(IRES-Neo).[8] The empty vector as a negative control was also introduced into Ba/F3 cells. As expected, the wild-type PDGFRA was not significantly phosphorylated on tyrosine residues in the absence of PDGF (Figure 1b). In contrast, the PDGFRA with the Ig5 domain A509D mutation was phosphorylated in the absence of PDGF (Figure 1b). Because the signal transduction pathway of PDGFRA is comparable with that of c-KIT,[2] the gain-of-function mutations of PDGFRA by themselves may transform Ba/F3 cells. In fact, Ba/F3 cells expressing the A509D mutant PDGFRA grew in the absence of IL-3 and PDGF whereas those expressing the wild-type did not (data not shown). It is possible that the mutant PDGFRA may contribute to leukemogenesis with t(4;11).

In conclusion, we reported the frequency of *PDGFRA* mutations in a large series of Japanese pediatric and infantile ALL patients. This is the first report showing a constitutively active *PDGFRA* mutation found in an ALL patient that may be associated with leukemic cell growth.

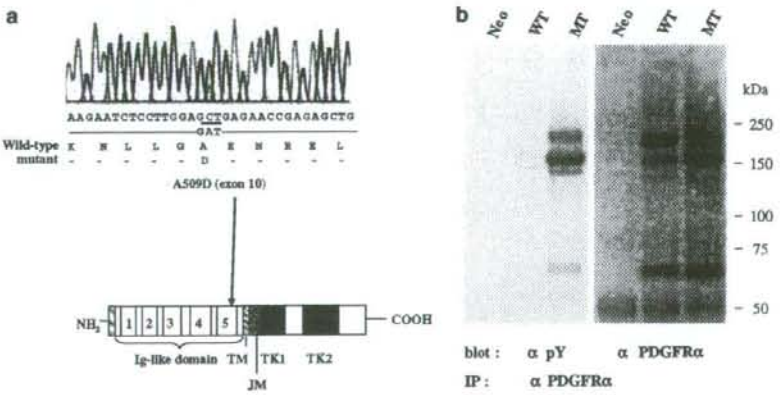

Figure 1 cDNA sequencing and position of the mutation of the *platelet-derived growth factor receptor α* (*PDGFRA*) gene at the Ig5 domain and tyrosine phosphorylation of the PDGFRA mutant. (**a**) Direct sequencing of the PCR product for the *PDGFRA* from an ALL patient with t(4;11) demonstrates the wild-type (WT) (top), and the A509D mutant (bottom) alleles. (**b**) Functional analysis of the WT PDGFRA and the A509D mutant derived from an ALL with t(4:11) patient. The mutant (MT), but not the WT PDGFRA was phosphorylated on tyrosine residues in Ba/F3 cells after retroviral transduction. Ba/F3 cells transduced with the empty vector (Neo) and those with the WT expressor were cultured with IL-3, and those with the MT expressor were cultured without IL-3. Lysates were prepared from cultured cells, immunoprecipitated with a polyclonal antibody to PDGFRA (sc-338, Santa Cruz Biotechnology, Santa Cruz, CA, USA), and immunoblotted with an anti-phosphotyrosine (pY) monoclonal antibody (Upstate Biotechnology, Inc., Lake Placid, NY, USA) (left panel), and with the anti-PDGFRA antibody (sc-338) (right panel). There was no detectable phosphorylation of WT PDGFRA. IP, immunoprecipitation. Ig, immunoglobulin; TM, transmembrane domain; JM, juxtamembrane domain; TK1 and TK2, two intracellular kinase domains.

Acknowledgements

We thank S Sohma and H Soga for technical assistance. We also thank Dr S Hirota for wild-type PDGFRA expression plasmid. This work was supported by a Grant-in-Aid for Cancer Research from the Ministry of Health, Labor, and Welfare of Japan, a Grant-in-Aid for Scientific Research on Priority Areas, and Grants-in-Aid from the Ministry of Education, Culture, Sports, Science and Technology of Japan.

M Hiwatari[1,4], R Ono[2,4], T Taki[3], A Hishiya[4], E Ishii[5], T Kitamura[4], Y Hayashi[6] and T Nosaka[2,4]

[1]*Department of Pediatrics, Graduate School of Medicine, The University of Tokyo, Tokyo, Japan;*
[2]*Department of Microbiology, Mie University Graduate School of Medicine, Tsu, Japan;*
[3]*Department of Molecular Laboratory Medicine, Kyoto Prefectural University of Medicine Graduate School of Medical Science, Kyoto, Japan;*
[4]*Division of Cellular Therapy, The Institute of Medical Science, The University of Tokyo, Tokyo, Japan;*
[5]*Department of Pediatrics, Ehime University Graduate School of Medicine, Ehime, Japan and*
[6]*Gunma Children's Medical Center, Gunma, Japan*
E-mail: nosaka@doc.medic.mie-u.ac.jp or hayashiy-tky@umin.ac.jp

References

1 Blume-Jensen P, Hunter T. Oncogenic kinase signalling. *Nature* 2001; **411**: 355–365.
2 Fletcher JA. Role of KIT and Platelet-Derived Growth Factor Receptors as Oncoproteins. *Seminars in Oncology* 2004; **31**: 4–11.
3 Hirota S, Nishida T, Isozaki K, Taniguchi M, Nakamura J, Okazaki T *et al.* Gain-of-function mutation at the extracellular domain of KIT in gastrointestinal stromal tumours. *Journal of Pathology* 2001; **193**: 505–510.
4 Tefferi1 A, Gilliland DG. Oncogenes in Myeloproliferative Disorders. *Cell Cycle* 2007; **5**: 550–566.
5 Hiwatari M, Taki T, Tsuchida M, Hanada R, Hongo T, Sako M *et al.* Novel missense mutations in the tyrosine kinase domain of the platelet-derived growth factor receptor alpha(PDGFRA) gene in childhood acute myeloid leukemia with t(8;21)(q22;q22) or inv(16)(p13q22). *Leukemia* 2005; **19**: 476–477.
6 Burgstaller S, Kreil S, Waghorn K, Metzgeroth G, Preudhomme C, Zoi K *et al.* The severity of *FIP1L1–PDGFRA*-positive chronic eosinophilic leukaemia is associated with polymorphic variation at the *IL5RA* locus. *Leukemia* 2007; **21**: 2428–2432.
7 Wang YY, Zhou GB, Yin T, Chen B, Shi JY, Liang WX *et al. AML1–ETO* and *C–KIT* mutation/overexpression in t(8;21) leukemia: Implication in stepwise leukemogenesis and response to Gleevec. *Proc Natl Acad Sci USA* 2005; **102**: 1104–1109.
8 Kitamura T, Koshino Y, Shibata F, Oki T, Nakajima H, Nosaka T *et al.* Retrovirus-mediated gene transfer and expression cloning: Powerful tools in functional genomics. *Exp Hematol* 2003; **31**: 1007–1014.

Clinical and biological significance of *RAS* mutations in multiple myeloma

Leukemia (2008) **22**, 2280–2284; doi:10.1038/leu.2008.142; published online 5 June 2008

Primary genetic abnormalities in myeloma (MM) such as trisomies of chromosomes 3, 5, 7, 9, 11, 15, 19 and 21 associated with hyperdiploid MM and translocations involving the immunoglobulin heavy chain (IgH) locus on chromosome 14q32 and three main recurrent partners: MMSET/FGFR3, CCND1 and c-MAF are already present in the pre-malignant monoclonal gammopathy of undetermined significance (MGUS) stage.[1] Some patients with these genetic abnormalities may remain as MGUS for many years without transforming to MM, suggesting that they are involved in clonal initiation but do not mediate malignant transformation.

One of the recurrent differences between MGUS and MM is the presence of *RAS* mutations in the latter. *RAS* mutations may, therefore, play an important role in malignant transformation of clonal plasma cells and myeloma pathogenesis. However, the clinical and biological significance of *RAS* mutation in MM has not been clearly established as most of the previous studies have involved small numbers of heterogeneously treated patients.

To establish the clinical and biological significance of *RAS* mutation in MM, we studied the association of *RAS* mutation with a comprehensive spectrum of clinical parameters including the newly established ISS staging and survival, as well as a panel of known recurrent genetic abnormalities in MM such as t(4;14), t(14;16), t(11;14), chromosome 13 and 17p13 deletion detected by fluorescent *in situ* hybridization[2] and ploidy assessed by DNA content measurement using flow cytometry,[3] in a large cohort of newly diagnosed patients enrolled in the Eastern Cooperative Group (ECOG) clinical trial E9486/E9487 ($N=561$).[4] A total of 439 patients, based on sample availability, were included (The ECOG Cohort). For this cohort, DNA from unsorted whole bone marrow was used for *RAS* mutation studies. We also studied 14 MGUS patients and 82 MM patients (60 newly diagnosed and 22 relapsed) from the Mayo Clinic (Mayo Cohort). Bone marrow samples were obtained after informed consent according to the Declaration of Helsinki. The study was approved by the Mayo Clinic Institution Review Board. CD138 positive plasma cells were enriched using immuno-magnetic beads (AutoMACS; Miltenyi-Biotec, Auburn, CA, USA). RNA and DNA from these enriched cells were used for gene expression and *RAS* mutation studies, respectively.

Conformation sensitive gel electrophoresis was used to screen samples for *KRAS* (codons 12, 13 and 61) and *NRAS* (codons 12, 13 and 61) mutations (Supplementary Methods). *RAS* mutation was detected in 102 (23%) patients in the ECOG cohort. Seventy-four (17%) patients had mutations in *NRAS*. The majority of these mutations were in codon 61 (64 of the 74), with 5 mutations detected in codons 12 and 13. We also found mutations in codon 64 ($n=1$) and codon 86 ($n=4$). Twenty-eight (6%) patients had mutations in K-*RAS*. Twenty-two of these are in codons 12 and 13 and three in codon 61. In addition, we also found one mutation each in codon 16, 22 and 24. In the Mayo Clinic cohort, *RAS* mutation was detected in 1 of 14 MGUS patients (7%), 15 of 60 newly diagnosed MM patients (25%) and 10 of 22 relapsed MM patients (45%). Once again N-*RAS* mutations were more common that K-*RAS* mutations. Our study confirms the low incidence of *RAS* mutation in MGUS compared to MM found in a previous study,[5] consistent with

ELSEVIER

Cancer Genetics and Cytogenetics 186 (2008) 115–119

CANCER GENETICS AND CYTOGENETICS

Short communication

MNX1–ETV6 fusion gene in an acute megakaryoblastic leukemia and expression of the *MNX1* gene in leukemia and normal B cell lines

Takeshi Taketani[a,b], Tomohiko Taki[c], Masahiro Sako[d], Takefumi Ishii[d], Seiji Yamaguchi[a], Yasuhide Hayashi[e,*]

[a]*Department of Pediatrics, Shimane University Faculty of Medicine, Izumo, Shimane, Japan*
[b]*Division of Blood Transfusion, Shimane University Hospital, Matsue, Shimane, Japan*
[c]*Department of Molecular Laboratory Medicine, Kyoto Prefectural University of Medicine Graduate School of Medical Science, Kyoto, Japan*
[d]*Department of Pediatric Hematology/Oncology, Osaka City General Hospital, Osaka, Japan*
[e]*Department of Hematology/Oncology, Gunma Children's Medical Center, 779 Shimohakoda, Hokkitsu, Shibukawa, Gunma 377-8577, Japan*

Received 5 March 2008; received in revised form 11 June 2008; accepted 27 June 2008

Abstract Patients with infant acute myeloid leukemia (AML) who carry a t(7;12)(q36;p13) translocation have been reported to have a poor clinical outcome. *MNX1–ETV6* fusion transcripts (previously *HLXB9–ETV6*) were rarely detected in AML patients having t(7;12)(q36;p13). A 23-month-old girl with acute megakaryoblastic leukemia (AMKL) exhibited chromosome abnormalities, including add(7)(q22), and del(12)(p12p13). Southern blot analysis of bone marrow cells showed an *ETV6* gene rearrangement. Reverse transcriptase-polymerase chain reaction (RT-PCR) followed by sequence analysis revealed the presence of an *MNX1–ETV6* fusion gene. The patient responded well to chemotherapy, achieved complete remission, and at writing had been in complete remission for 60 months. The *MNX1* expression by RT-PCR was significantly more frequent in Epstein–Barr virus–transformed B-cell lines derived from normal adult lymphocytes than in leukemic cell lines. This represents a novel case of an AMKL patient with *MNX1–ETV6* fusion transcripts who had a good prognosis.

1. Introduction

Many recurrent chromosomal translocations are involved in acute myeloid leukemia (AML) [1]. AML with 12p13 translocations have been reported to involve the ETS variant gene 6 (*TEL* oncogene) (*ETV6*) [2]. In cases of AML carrying 12p13 abnormalities, a recurrent translocation t(7;12)(q36;p13) is found in 20%–30% of infant cases [3–5]. Fluorescence in situ hybridization assay is needed to evaluate this translocation, because it is difficult to detect by conventional karyotyping [3–5]. AML patients with this translocation are characterized by age under 20 months at diagnosis, thrombocytosis, high percentage of CD34-positive cells, presence of additional chromosomal abnormalities, including trisomy 19 or trisomy 8 (or both), and a poor prognosis [3–5]. An *MNX1–ETV6* fusion gene (previously *HLXB9–ETV6*) was identified in two pediatric AML patients having t(7;12)(q36;p13) [6]; however, heterogeneity of the 7q36 and 12p13 translocations was reported [5,7,8]. Thus, *MNX1–ETV6* fusion gene in AML patients having t(7;12) is infrequently reported [7,8].

We describe the case of a 23-month-old AML patient with add(7)(q22), del(12)(p12p13), and *MNX1–ETV6* fusion transcript; the child has remained alive for 5 years. We also report the expression of the *MNX1* gene in several leukemic and normal Epstein–Barr virus-transformed cell lines.

2. Case report

A 23-month-old girl was admitted to Osaka City General Hospital because of appetite loss and pallor. Blood examination showed a white blood cell count of 10,520/μL with 55.5% blasts, a hemoglobin level of 7.0 g/dL, and a platelet count of 164,000/μL. She had a mediastinal mass, but no hepatosplenomegaly. Bone marrow examination revealed a nuclear cell count of 30,000/μL with 71.2% blasts. The

* Corresponding author. Tel.: +81-279-52-3551, ext. 2200; fax: +81-279-52-2045.
E-mail address: hayashiy-tky@umin.ac.jp (Y. Hayashi).

0165-4608/08/$ – see front matter
doi:10.1016/j.cancergencyto.2008.06.009

blasts were negative for myeloperoxidase staining and platelet peroxidase staining electron-microscopically. Flow cytometric analysis showed that the blasts expressed CD41, CD36, CD13, CD33, CD15, and CD7 antigens, suggesting megakaryoblastic origin. Conventional G-banding chromosomal analysis revealed a karyotype of 46,XX,add (7)(q22),del(12)(p12p13) in all 20 bone marrow cells examined (Fig. 1).

The patient was diagnosed as having AMKL (M7 subtype, based on the French–American–British classification), and was treated on the Japanese Childhood AML Cooperative Study Group Protocol, AML99 [9]. She obtained complete remission with induction chemotherapy (cytarabine, etoposide, and mitoxantrone). Thereafter, she was treated with five additional courses of intensive chemotherapy (high-dose cytarabine, etoposide, idarubicin, and mitoxantrone). As of writing, she had been in complete remission for 60 months after diagnosis.

3. Materials and methods

3.1. Southern blot analysis

High molecular weight DNA was extracted from bone marrow cells of the patient by proteinase K digestion and phenol–chloroform extraction [10]. Ten micrograms of DNA was digested with *Eco*RI, subjected to electrophoresis on 0.7% agarose gels, and transferred to nylon membrane, and hybridized to cDNA probes ^{32}P-labeled by the random hexamer method [10]. The probes used were a 516-bp *MNX1* cDNA fragment (nucleotide nt598 to nt1114; GenBank accession no. NM_005515; previously *HLXB9*).

3.2. Expression of WT1 mRNA and mutation of FLT3

WT1 mRNA was examined for detection of minimal residual disease as previously reported [11]. Internal tandem duplication and mutation of *FLT3* were examined as previously reported [10].

3.3. Reverse transcriptase–polymerase chain reaction and nucleotide sequencing

MNX1–ETV6 chimeric mRNA was detected by reverse transcriptase–polymerase chain reaction (RT-PCR) as described previously [12]. Total RNA was extracted from the leukemic cells of the patient using the acid guanidine thiocyanate–phenol chloroform method [12]. Total RNA (4 μg) was reverse-transcribed to cDNA, using a cDNA synthesis kit (GE Healthcare Bio-Science, Piscataway, NJ) [12]. PCR was performed with AmpliTaq Gold DNA polymerase (Applied Biosystems, Foster City, CA; Tokyo, Japan), using the reagents recommended by the manufacturer. The primers used and PCR conditions were as described previously [6]. The PCR products were subcloned into pCR2.1 vector (Invitrogen, Carlsbad, CA) and sequenced by the fluorometric method using the BigDye Terminator cycle sequencing kit (Applied Biosystems).

3.4. Expression of the MNX1 gene by RT-PCR in leukemic cell lines

To analyze the expression pattern of the *MNX1* gene in leukemic cell lines, RT-PCR was performed. Fifty-nine cell lines were examined, as follows [12]; 10 B-precursor ALL cell lines (LC4-1, NALM-6, NALM-24, NALM-26, UTP-2, RS4;11, SCMC-L10, KOCL-33, KOCL-45, KOCL-69), 9

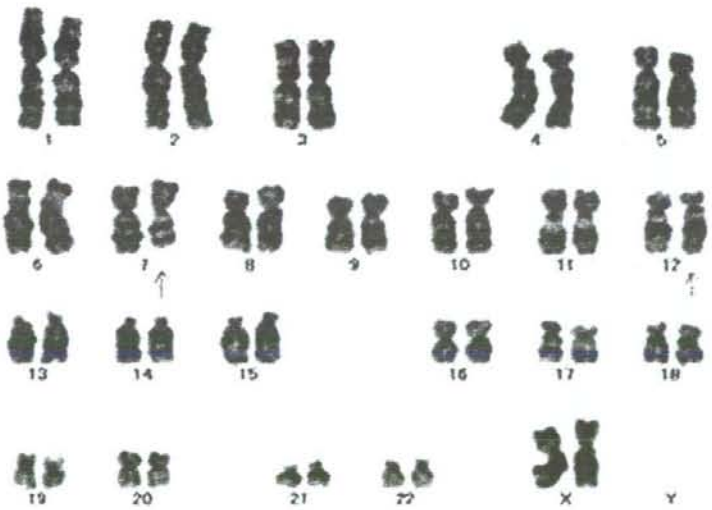

Fig. 1. G-banding karyotype of the leukemic cells in a pediatric patient with acute megakaryoblastic leukemia: 46,XX,add(7)(q22),del(12)(p12p13).

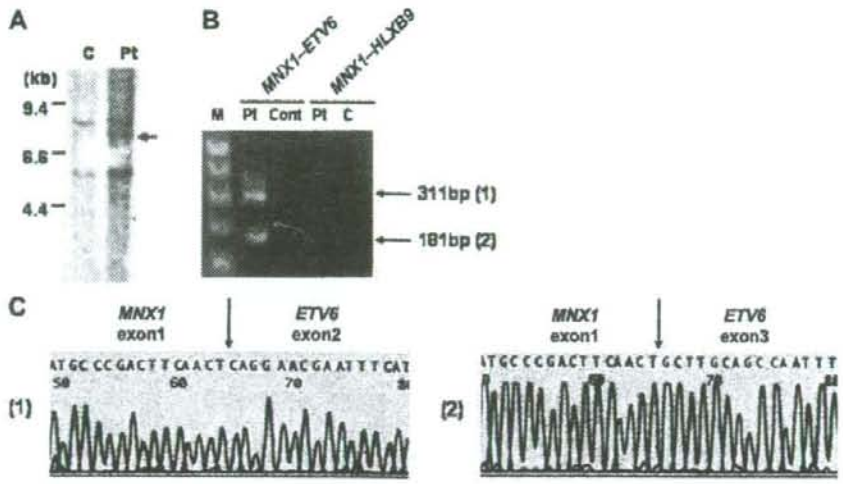

Fig. 2. Detection of the *MNX1–ETV6* fusion gene (previously *HLXB9–ETV6*). (A) Rearrangement of the *MNX1* gene by Southern blotting with *Eco*RI digestion. The arrow indicates a rearranged band of the *MNX1* gene; C, control; Pt, patient. (B) The *MNX1–ETV6* fusion transcript identified by reverse transcriptase–polymerase chain reaction (RT-PCR). Lanes 2 and 3, *MNX1–ETV6* fusion transcript; lanes 4 and 5, *ETV6–MNX1* fusion transcript. C, control; M, size marker; Pt, patient; (C) Nucleotide and amino acid sequencing of two *MNX1–ETV6* fusion transcripts.

B-ALL cell lines (BALM-1, BALM-13, BALM-14, BJAB, DAUDI, RAJI, RAMOS, BAL-KH, NAMALLA), 9 T-ALL cell lines (RPMI-8402, MOLT-14, THP-6, PEER, H-SB2, HPB-ALL, L-SAK, L-SMY, KCMC-T), 8 AML cell lines (YNH-1, ML-1, KASUMI-3, KG-1, inv-3, SN-1, NB4, HEL), 6 acute monocytic leukemia cell lines (THP-1, IMS/M1, CTS, P31/FUJ, MOLM-13, KOCL-48), 5 chronic myelogenous leukemia cell lines (MOLM-1, MOLM-7, TS9;22, SS9;22, K-562), 2 acute megakaryoblastic leukemia cell lines (CMS, CMY), and 10 Epstein-Barr virus transformed B lymphocyte (EBV-B) cell lines derived from normal adult peripheral lymphocytes. Five normal BM samples were also examined. RT-PCR mixtures and conditions were the same as described [10]. The primers used for RT-PCR were HLXB9-658F (5′-GGCATGATCCTGCCTAAGAT-3′) (sense primer) and HLXB9-1092R (TGCT GTAGGGGAAATGGTCGTCG) (antisense primer) [6].

4. Results and discussion

The karyotype of the patient's leukemic cells was 46,XX,add(7)(q22),del(12)(p12p13), suggesting that both *ETV6* and *MNX1* were involved in this chromosomal abnormality. With informed consent from the patient's parents, DNA and total RNA were extracted from bone marrow cells of the patient. Southern blot analysis of DNA from leukemic cells of the patient using the *MNX1* probe showed a rearranged band (Fig. 2A). We performed RT-PCR for *MNX1–ETV6* chimeric mRNA and obtained two RT-PCR products, of 311 bp and 181 bp (Fig. 2B). Sequence analysis of these PCR products showed that one product was an in-frame fusion transcript of exon 1 of *MNX1* to exon 3 of *ETV6*, and the other was an out-of-frame fusion transcript of exon 1 of *MNX1* to exon 2 of *ETV6* (Fig. 2C). These transcripts were the same as previously reported [6]. The reciprocal *ETV6–MNX1* transcript was not detected (Fig. 2B).

The *WT1* mRNA level was 3,400 copies/μg RNA at diagnosis, but decreased to <50 copies/μg RNA after remission. Neither internal tandem duplication nor mutation of *FLT3* were found in this patient, suggesting that the prognosis is not poor [1].

Table 1
Expression of the *MNX1* gene in leukemia and EBV-B cell lines by reverse transcriptase–polymerase chain reaction

Cell line	Cells examined, no.	Cells expressing *MNX1*, no. (%)
ALL	28	5 (17.9)
B precursor	10	0 (0)
B	9	2 (22.2)
T	9	3 (33.3)
AML	16	3 (18.8)
AML	8	1 (12.5)
AMoL	6	2 (33.3)
AMKL	2	0 (0)
CML	5	1 (20)
EBV-B	10	7 (70)
normal BM	5	0 (0)

Abbreviations: ALL, acute lymphoblastic leukemia; AMKL, acute megakaryoblastic leukemia; AML, acute myeloid leukemia; AMoL, acute monocytic leukemia; B, B-cell; BM, bone marrow; CML, chronic myelogenous leukemia; EBV-B, Epstein–Barr virus-transformed human B lymphocytes; T, T-cell.

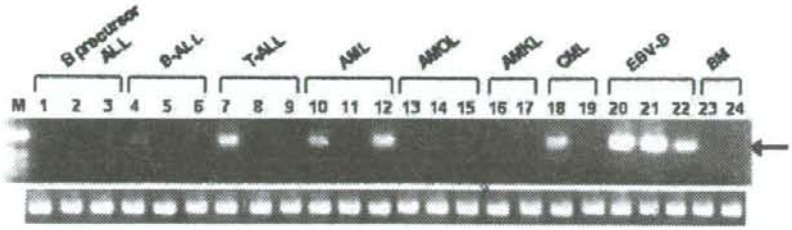

Fig. 3. Expression of the *MNX1* gene in leukemia and EBV-B cell lines by RT-PCR. ALL, acute lymphoblastic leukemia; AMKL, acute megakaryoblastic leukemia; AML, acute myeloid leukemia; AMOL, acute monocytic leukemia; B, B-cell; BM, bone marrow; CML, chronic myelogenous leukemia; EBV-B, Epstein–Barr virus-transformed human B lymphocytes; T, T-cell.

We next examined the *MNX1* expression by RT-PCR analysis in 49 leukemic cell lines, and 10 EBV-B cell lines. *MNX1* was not frequently expressed in lymphoid or myeloid leukemic cell lines (Table 1; Fig. 3). *MNX1* was expressed in 7 of 10 EBV-B cell lines, but not in 5 normal BM cells. The *MNX1* expression was significantly more frequent in EBV-B cell lines than in leukemic cell lines ($P = 0.0015$) or in normal BM cells ($P = 0.0256$). The *MNX1* was frequently expressed in CD34-positive cells purified from normal BM cells, acute leukemia cells, and AML cells having t(7;12)(q36;p13) [5,13,14]. It is unknown whether the incidence of *MNX1* expression differs among leukemia cell lines. Mature B-lineage cells are likely to frequently express *MNX1* transcripts, and the transcripts were more prevalent in several human B lineage cell line and tonsil B cells [15]. The present findings are compatible with previous reports. *MNX1* may be associated with differentiation of B cells.

MNX1–ETV6 fusion transcript has so far been detected in only four out of the many AML patients who carry the t(7;12) anomaly [5,6]. Difficulty of detection of this fusion transcript is due to breakpoint heterogeneity of the 7q36 and 12p13 in this translocation [7,8]. Clinical features of AML patients having t(7;12) did not differ between the presence and absence of *MNX1–ETV6* fusion transcripts [5]. Notably, clinical characteristics of the present patient were different from those of AML patients having t(7;12) previously reported. Our patient was diagnosed as having AMKL, although most AML patients having t(7;12) were identified as poorly differentiated FAB subtypes [5]. Only one patient was reported to be diagnosed with AMKL; however, *MNX1–ETV6* fusion transcript was not examined in that case [4]. An additional cytogenetic abnormality is trisomy 19 [3–5]. Chromosomal analysis of the present patient showed absence of additional chromosomal abnormalities, suggesting long-term disease-free survival with chemotherapy alone. All AML patients, except one who had both t(7;12) and trisomy 19, died [3–6]. These findings suggest that t(7;12) is associated only with leukemogenesis, and that other factors including trisomy 19 and *FLT3* mutations, may affect the prognosis of AML patients having t(7;12).

In conclusion, an AMKL patient with *MNX1–ETV6* fusion transcripts had a good prognosis. Further accumulation of clinical and molecular data of AML patients having t(7;12) is needed to clarify this result.

Acknowledgments

We express our appreciation to Mrs. Shoko Sohma and Hisae Soga for their excellent technical assistance. We thank Dr. Takeyuki Sato, Department of Pediatrics, Chiba University School of Medicine, Japan, for providing AMKL (CMS, CMY) cell lines; Dr. Kanji Sugita, Department of Pediatrics, Yamanashi University School of Medicine, Japan, for providing ALL (KOCL-33, -45, -69) cell lines and AMoL (KOCL-48) cell lines; and Dr. Yoshinobu Matsuo, Hayashibara Biochemical Laboratories, Inc., Fujisaki Cell Center, Japan, for providing varieties of ALL cell lines. This work was supported by a Grant-in-Aid for Cancer Research, Research on Children and Families from the Ministry of Health, Labor, and Welfare of Japan, a Grant-in-Aid for Scientific Research (C), and Exploratory Research from the Ministry of Education, Culture, Sports, Science, and Technology of Japan.

References

[1] Hayashi Y. The molecular genetics of recurring chromosome abnormalities in acute myeloid leukemia. Semin Hematol 2000;37:368–80.

[2] Bohlander SK. *ETV6*: a versatile player in leukemogenesis. Semin Cancer Biol 2005;15:162–74.

[3] Tosi S, Harbott J, Teigler-Schlegel A, Haas OA, Pirc-Danoewinata H, Harrison CJ, Biondi A, Cazzaniga G, Kempski H, Scherer SW, Kearney L. t(7;12)(q36;p13), a new recurrent translocation involving *ETV6* in infant leukemia. Genes Chromosomes Cancer 2000;29:325–32.

[4] Slater RM, von Drunen E, Kroes WG, Weghuis DO, van den Berg E, Smit EM, van der Does-van den Berg A, van Wering E, Hählen K, Carroll AJ, Raimondi SC, Beverloo HB. t(7;12)(q36;p13) and t(7;12)(q32;p13): translocations involving *ETV6* in children 18 months of age or younger with myeloid disorders. Leukemia 2001;15:915–20.

[5] von Bergh AR, van Drunen E, van Wering ER, van Zutven LJ, Hainmann I, Lönnerholm G, Meijerink JP, Pieters R, Beverloo HB.

High incidence of t(7;12)(q36;p13) in infant AML but not in infant ALL, with a dismal outcome and ectopic expression of *HLXB9*. Genes Chromosomes Cancer 2006;45:731–9.

[6] Beverloo HB, Panagopoulos I, Isaksson M, van Wering E, van Drunen E, de Klein A, Johansson B, Slater R. Fusion of the homeobox gene *HLXB9* and the *ETV6* gene in infant acute myeloid leukemias with the t(7;12)(q36;p13). Cancer Res 2001;61:5374–7.

[7] Simmons HM, Oseth L, Nguyen P, O'Leary M, Conklin KF, Hirsch B. Cytogenetic and molecular heterogeneity of 7q36/12p13 rearrangements in childhood AML. Leukemia 2002;16:2408–16.

[8] Tosi S, Hughes J, Scherer SW, Nakabayashi K, Harbott J, Haas OA, Cazzaniga G, Biondi A, Kempski H, Kearney L. Heterogeneity of the 7q36 breakpoints in the t(7;12) involving *ETV6* in infant leukemia. Genes Chromosomes Cancer 2003;38:191–200.

[9] Shimada A, Taki T, Tabuchi K, Tawa A, Horibe K, Tsuchida M, Hanada R, Tsukimoto I, Hayashi Y. *KIT* mutations, and not *FLT3* internal tandem duplication, are strongly associated with a poor prognosis in pediatric acute myeloid leukemia with t(8;21): a study of the Japanese Childhood AML Cooperative Study Group. Blood 2006;107:1806–9.

[10] Taketani T, Taki T, Sugita K, Furuichi Y, Ishii E, Hanada R, Tsuchida M, Sugita K, Ida K, Hayashi Y. *FLT3* mutations in the activation loop of tyrosine kinase domain are frequently found in infant ALL with *MLL* rearrangements and pediatric ALL with hyperdiploidy. Blood 2004;103:1085–8.

[11] Inoue K, Ogawa H, Yamagami T, Soma T, Tani Y, Tatekawa T, Oji Y, Tamaki H, Kyo T, Dohy H, Hiraoka A, Masaoka T, Kishimoto T, Sugiyama H. Long-term follow-up of minimal residual disease in leukemia patients by monitoring *WT1* (Wilms tumor gene) expression levels. Blood 1996;88:2267–78.

[12] Taketani T, Taki T, Shibuya N, Kikuchi A, Hanada R, Hayashi Y. Novel *NUP98–HOXC11* fusion gene resulted from a chromosomal break within exon 1 of *HOXC11* in acute myeloid leukemia with t(11;12)(p15;q13). Cancer Res 2002;62:4571–4.

[13] Deguchi Y, Kehrl JH. Selective expression of two homeobox genes in CD34-positive cells from human bone marrow. Blood 1991;78: 323–8.

[14] Deguchi Y, Yamanaka Y, Theodossiou C, Najfeld V, Kehrl JH. High expression of two diverged homeobox genes, HB24 and HB9, in acute leukemias: molecular markers of hematopoietic cell immaturity. Leukemia 1993;7:446–51.

[15] Harrison KA, Druey KM, Deguchi Y, Tuscano JM, Kehrl JH. A novel human homeobox gene distantly related to proboscipedia is expressed in lymphoid and pancreatic tissues. J Biol Chem 1994;269: 19968–75.

Hemophagocytic Lymphohistiocytosis Associated With Uncontrolled Inflammatory Cytokinemia and Chemokinemia was Caused by Systemic Anaplastic Large Cell Lymphoma: A Case Report and Review of the Literature

To the Editor:

Hemophagocytic syndrome or hemophagocytic lymphohistiocytosis (HLH) induced by lymphoma has been reported in Asian adult patients and was called lymphoma-associated hemophagocytic syndrome.[1,2] However, lymphoma-associated hemophagocytic syndrome was rarely reported in adults and children of Western countries.[3] Especially, HLH associated with anaplastic large-cell lymphoma (ALCL) was well known, but uncertain in pathophysiology and rarely reported in children.[4] On the other hand, anaplastic large kinase (ALK)-positive ALCL was predominant in children and young adults. ALK-positive ALCL showed a better prognosis than ALK-negative ALCL.[5] We present here a case of a 3-year-old boy with HLH who suffered from systemic ALCL. No family history of immunodeficiency was observed. He showed prolonged fever, pleural effusion, liver dysfunction, and pancytopenia. The extranodular diseases including brain, lung, skin, liver, and soft tissue were observed by magnetic resonance imaging (Fig. 1A). Bone marrow picture showed the erythrophagocytosis. The biopsy of lymph node showed the aggregation of large cells positively stained by antibodies of CD30 or ALK. The karyotypic analysis showed t(2;5)(p23;q35) by G-banding method and the transcript of *NPM-ALK* was confirmed by real-time–polymerase chain reaction (RT-PCR) and direct sequencing (data not shown). Bone marrow sample also showed the transcript of *NPM-ALK* by real-time–PCR from the first diagnosis. The infections of Epstein-Barr virus or cytomegalovirus were denied by PCR analysis. The disease was severe and fatal compared with ALCL without HLH. Systemic chemotherapy for ALCL with immunosuppressive therapy using steroid and cyclosporine were repeatedly

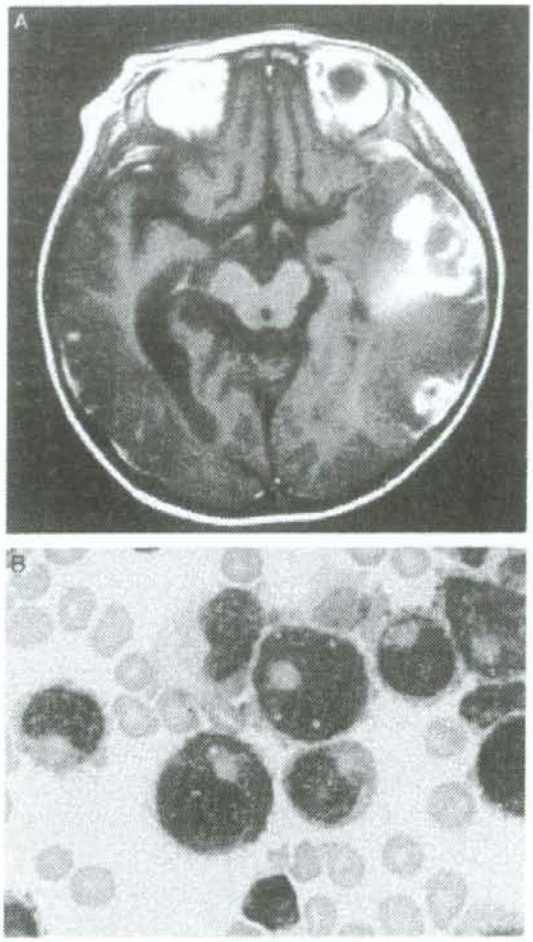

FIGURE 1. A, A gadolinium-enhanced MRI imaging of the brain. High-intensity area was estimated to be the invaded lesion by tumor cells. B, A picture of May-Giemsa staining of cytospine of cerebrospinal fluid. Tumor cells were observed. MRI indicates magnetic resonance imaging.

Supported in part by a Grant-in-Aid for Cancer Research, a Grant for Clinical Cancer Research and Research on Children and Families from the Ministry of Health, Labor, and Welfare of Japan. Supported also by Grant-in-Aid for Scientific Research (C) from the Ministry of Education, Culture, Sports, Science, and Technology of Japan and Research Grant for Gunma Prefectural Hospitals.

continued; however, the chemotherapy had only the transient effect for this patient and continuous hemodiafiltration was needed. However, the disease progressed and the ALK-positive cells were finally detected even in peripheral blood and cerebrospinal fluid (Fig. 1B). He died after 6 months of diagnosis.

We analyzed 23 cytokines and chemokines in patient's sera to explain the pathophysiology of HLH in this case using the multiplex suspension array system (BioLad Laboratories).[6] The several proinflammatory cytokines and chemokines were vastly elevated in this patient's sera, especially, interleukin (IL)-1β, IL-2, IL-6, IL-7, IL-15, interferon-γ, interferon-inducible protein-10, macrophage inflammatory protein-1α, and macrophage inflammatory protein-1β were elevated significantly compared with those in control sera from 10 healthy children (Table 1). Furthermore, repeated chemotherapy and immunosuppressive therapy were continued, the cytokines and chemokines levels did not change significantly, and repeated high fever, hyperferritinemia, and liver dysfunction were continued.

There was a report about ALCL cell line, HSC-M1, which was established from a 5-year-old girl who suffered from ALCL and erythrophagocytosis, that was reported to produce several cytokines.[7] Other reports also suggested the production of several cytokines by tumor cells of ALCL without HLH.[8,9] We suspected that the cytokines and chemokines in this case were produced by systemic ALK-positive cells and accessory cells. These abnormal cytokines and chemokines affected the prognosis as reported by a Japanese lymphoma study on adults.[2]

Furthermore, we suspected the possibility of immunodeficiency in this patient because of the unusual clinical course of ALCL. Clementi et al[10] reported 4 patients with non-Hodgkin lymphoma with features of HLH who had mutations in the perforin (*PRF1*) gene, which was estimated as the causative gene for familial hemophagocytic syndrome. We analyzed the exon 2 and 3 of *PRF1* gene in this case but we could

TABLE 1. Cytokines and Chemokines in Sera of Patients and Controls

	IL-1β	IL-1Rα	IL-2	IL-6	IL-7	IL-15	Eotaxin	bFGF	IFN-γ	IP-10	MCP-1 (MCAF)	MIP-1α	MIP-1β
At diagnosis	3.24	2194.54	7.84	30.18	6.89	3.38	33.76	25.91	205.6	6861.41	14.37	4.46	49.27
After chemotherapy-1	7.02	2304.08	9.13	181.81	3.25	71.8	104.7	11.51	195.76	16266.03	937.87	8.54	100.49
After chemotherapy-2	2.38	403.32	10.05	54.49	9.82	25.71	116.37	0.01	136.05	22673.56	145.16	5.37	350.38
After chemotherapy-3	3.42	130.51	0.01	25.65	5.1	0.01	81.19	0.01	84.27	7428.93	55.67	5.56	123.43
Mean ± SD (patient)	4.02 ± 2.10	1258.11 ± 1150.8	6.76 ± 4.60	73.03 ± 73.62	6.27 ± 2.80	25.23 ± 33.10	84.0 ± 36.55	9.36 ± 12.30	155.42 ± 56.52	13507.48 ± 7584.76	288.27 ± 436.50	5.98 ± 1.77	1.58 ± 3.14
Mean ± SD (controls)	1.72 ± 0.57	11.26 ± 14.56	0.061 ± 0.16	1.29 ± 2.40	2.50 ± 0.98	0.01 ± 0.0	32.65 ± 36.53	0.01 ± 0.0	18.75 ± 22.92	230.17 ± 95.75	3.84 ± 2.75	0.01 ± 0.0	45.81 ± 18.94
P	0.0016	0.0033	0.0004	0.0065	0.0006	0.0242	0.035	0.0245	< 0.0001	< 0.0001	0.0476	< 0.0001	0.0189

We analyzed the serum cytokine and chemokines at 4 points. These points were as follows, first point was at diagnosis and the other 3 points were after the repeated chemotherapy, respectively.
Controls sera were obtained from 10 healthy children.
bFGF indicates basic fibroblast growth factor; IFN, interferon; IL, interleukin; IP, interferon-inducible protein; MCAF, monocyte chemotactic and activating factor; MCP, monocyte chemotactic protein; MIP, macrophage inflammatory protein.

not find the mutation. We also analyzed signaling lymphocytic activation molecule-associated protein (*SAP*) gene, which was estimated as the causative gene for X-linked lymphoproliferative syndrome, but no mutation was detected. ALCL was considered to be a heterogeneous disease, and recently, the activation of janus kinase 3 (JAK3)/signal transducer and activator of transcription 3 (JAK3/STAT3) pathway was observed.[8] We must await further study to investigate the different molecular mechanism of ALCL with or without HLH and hypercytokinemia.

Akira Shimada, MD, PhD*
Masahiko Kato, MD, PhD†
Kazushi Tamura, MD, PhD‡
Junko Hirato, MD, PhD§
Hirokazu Kanegane, MD, PhD‖
Yasuhiko Takechi, MD*
Myoung-ja Park, MD*
Manabu Sotomatsu, MD, PhD*
Shinitsu Hatakeyama, MD, PhD¶
Yasuhide Hayashi, MD, PhD*
Departments of *Hematology/Oncology
†Allergy and Immunology
¶Radiology, Gunma Children's Medical Center, Hokittsu, Shibukawa
Departments of ‡Pediatrics
§Pathology, Gunma University, Graduate School of Medicine, Gunma
‖Department of Pediatrics
Graduate School of Medicine
University of Toyama
Toyama, Japan

REFERENCES

1. Shimazaki C, Inaba T, Okano A, et al. Clinical characteristics of B-cell lymphoma-associated hemophagocytic syndrome (B-LAHS): comparison of CD5+ with CD5- B-LAHS. *Intern Med.* 2001;40:878–882.
2. Ohno T, Ueda Y, Nagai K, et al, Kyoto University Hematology/Oncology Study Group. The serum cytokine profiles of lymphoma-associated hemophagocytic syndrome: a comparative analysis of B-cell and T-cell/natural killer cell lymphomas. *Int J Hematol.* 2003;77:286–294.
3. Blatt J, Weston B, Belhorn T, et al. Childhood non-Hodgkin lymphoma presenting as hemophagocytic syndrome. *Pediatr Hematol Oncol.* 2002;19:45–49.
4. Krenova Z, Sterba J, Blatny J, et al. A case of anaplastic large cell lymphoma-induced hemophagocytic lymphohistiocytosis in an adolescent female. *Pediatr Blood Cancer.* 2007;49:1056.
5. Stein H, Foss HD, Durkop H, et al. CD30(+) anaplastic large cell lymphoma: a review of its histopathologic, genetic, and clinical features. *Blood.* 2000;96:3681–3695.
6. Shimada A, Hayashi Y, Ogasawara M, et al. Pro-inflammatory cytokinemia is frequently found in Down syndrome patients with hematological disorders. *Leuk Res.* 2007;31:1199–1203.
7. Al-Hashmi I, Decoteau J, Gruss HJ, et al. Establishment of a cytokine-producing anaplastic large-cell lymphoma cell line containing the t(2;5) translocation: potential role of cytokines in clinical manifestations. *Leuk Lymphoma.* 2001;40:599–611.
8. Qiu L, Lai R, Lin Q, et al. Autocrine release of interleukin-9 promotes JAK3-dependent survival of ALK+ anaplastic large-cell lymphoma cells. *Blood.* 2006;108:2407–2415.
9. Siebert S, Amos N, Williams BD, et al. Cytokine production by hepatic anaplastic large-cell lymphoma presenting as a rheumatic syndrome. *Semin Arthritis Rheum.* 2007;37:63–67.
10. Clementi R, Locatelli F, Dupre L, et al. A proportion of patients with lymphoma may harbor mutations of the perforin gene. *Blood.* 2005;105:4424–4428.

Successful use of Alemtuzumab in a Child With Refractory Peripheral T-cell Posttransplant Lymphoproliferative Disorder

To the Editor:

Posttransplant lymphoproliferative disorder (PTLD) is a well-known complication of solid organ transplantation in children. The majority of PTLD cases develop early from Epstein-Barr virus (EBV)-infected B lymphocytes.[1,2] In contrast, T-cell PTLD comprises 50% to 70% of late-onset PTLD, is often peripheral (mature) T-cell subtype and EBV-negative.[3] We report successful use of alemtuzumab in a child with refractory T-cell PTLD.

A 20-month-old girl presented at 17 months postcardiac transplant with retroperitoneal, mesenteric, and mediastinal lymphadenopathy, and bowel wall thickening. She had received tacrolimus and mycophenolate as posttransplant immunosuppression. Complete blood count showed a haemoglobin of 128 g/L, white blood cells of 38.3 with lymphocytes of 24.5×10^9/L, and platelets of 140×10^9/L. Gastrointestinal biopsies, peripheral blood (PB) and bone marrow (BM) showed CD4-positive T cells expressing T-cell receptor vβ2 antigen, consistent with monoclonal T-cell population. The biopsies and PB were EBV-negative. A diagnosis of posttransplant EBV-negative monoclonal peripheral T-cell lymphoma/leukemia was made. Initially, she had good clinical response to a 4-drug induction chemotherapy (vincristine/daunorubicin/polyethylene glycol-asparaginase/prednisone) regimen, with disappearance of her diarrhea and weight gain. However, at the end of induction she still had PB and BM molecular disease and her symptoms recurred. Therefore, she received FLAG (fludarabine at 30 mg/m^2/d for 4 d, high-dose cytarabine at 2 g/m^2/d for 4 d, and granulocyte colony-stimulating factor) chemotherapy, after which she had a brief clinical response and minimal radiographic improvement but with persistence of the molecular clone. Her fever and diarrhea recurred soon after, therefore, she was started on alemtuzumab (0.2 mg/kg) 3 times a week for 4 weeks, plus 3 doses of intravenous methotrexate (1 gm/m^2/wk) and daily oral 6-mercaptopurine. She rapidly achieved radiologic and molecular remission, and was later referred for allogeneic stem cell transplant (SCT) in view of initial refractoriness of the disease. She continued on alemtuzumab (0.2 mg/kg) twice weekly while waiting for SCT. She tolerated the alemtuzumab well without significant adverse effects. She underwent unrelated cord SCT with busulfan, cytarabine, melphalan, and alemtuzumab conditioning, and remains in complete remission at 4 months after her SCT.

Pediatric T-cell PTLD is rare, with only 19 cases previously reported. It is usually EBV-negative, monoclonal, and carries a poor prognosis.[2] There is no single effective chemotherapy regimen to treat these

Oncogene (2008) 27, 6749–6760

www.nature.com/onc

ORIGINAL ARTICLE

C/EBPα and C/EBPε induce the monocytic differentiation of myelomonocytic cells with the *MLL*-chimeric fusion gene

H Matsushita[1], H Nakajima[2], Y Nakamura[3], H Tsukamoto[3], Y Tanaka[1], G Jin[1], M Yabe[1], S Asai[1], R Ono[4], T Nosaka[4], K Sugita[5], A Morimoto[6], Y Hayashi[7], T Hotta[8], K Ando[8] and H Miyachi[1]

[1]*Department of Laboratory Medicine, Tokai University School of Medicine, Kanagawa, Japan;* [2]*Center of Excellence, Institute of Medical Science, University of Tokyo, Tokyo, Japan;* [3]*Teaching and Research Support Center, Tokai University School of Medicine, Kanagawa, Japan;* [4]*Department of Microbiology, Mie University Graduate School of Medicine, Mie, Japan;* [5]*Department of Pediatrics, School of Medicine, University of Yamanashi, Yamanashi, Japan;* [6]*Department of Pediatrics, Kyoto Prefectural University of Medicine, Graduate School of Medical Science, Kyoto, Japan;* [7]*Department of Hematology/Oncology, Gunma Children's Medical Center, Gunma, Japan and* [8]*Department of Hematology, Tokai University School of Medicine, Kanagawa, Japan*

CCAAT/enhancer binding proteins (C/EBPs) have an important function in granulocytic differentiation, and are also involved in the leukemogenesis of acute myeloid leukemia (AML). Their involvement in myelomonocytic leukemia, however, is still unclear. Therefore, the expression and function of C/EBPs in myelomonocytic cells with *MLL*-fusion genes were investigated. Retinoic acid (RA) induced monocytic differentiation in the myelomonocytic cell lines with *MLL*-fusion genes, THP-1, MOLM-14 and HF-6 cells, accompanied by monocytic differentiation with the upregulation of C/EBPα and C/EBPε. Monocytic differentiation by RA treatment was confirmed in primary AML cells using a clonogenic assay. When the activity of C/EBPα or C/EBPε was introduced into HF-6 cells, their cellular growth was arrested through differentiation into monocytes with the concomitant marked downregulation of *Myc*. *Cebpe* mRNA was upregulated by the induction of C/EBPα-ER, but not vice versa, thus suggesting that C/EBPε may have an important function in the differentiation process. Introduction of Myc isoforms into HF-6 cells partially antagonized the C/EBPs effects. These findings suggest that the ectopic expression of C/EBPε, as well as C/EBPα, can induce the monocytic differentiation of myelomonocytic leukemic cells with *MLL*-fusion gene through the downregulation of *Myc*, thus providing insight into the development of novel therapeutic approaches.
Oncogene (2008) **27**, 6749–6760; doi:10.1038/onc.2008.285; published online 8 September 2008

Keywords: acute myeloid leukemia; mixed lineage leukemia gene; monocytic differentiation; CCAAT/enhancer binding protein-α; CCAAT/enhancer binding protein-ε

Correspondence: Dr H Matsushita, Department of Laboratory Medicine, Tokai University School of Medicine, 143 Shimokasuya, Isehara, Kanagawa 259-1193, Japan.
E-mail: hmatsu@is.icc.u-tokai.ac.jp
Received 8 May 2007; revised 10 June 2008; accepted 8 July 2008; published online 8 September 2008

Introduction

Recurrent translocations involving the mixed lineage leukemia (*MLL*) gene located on chromosome 11q23 frequently occur in various hematological malignancies including acute myeloid leukemia (AML). In the translocations, truncated N-terminal MLL proteins with AT hooks and MT domain are fused in-frame to one of more than 40 translocation partners to produce proteins with novel properties. The translocation partners share little sequence homology, but the resultant chimeric proteins are thought to alter the transcription on MLL target genes (Li *et al.*, 2005).

Rearrangements involving 11q23 or *MLL* are found in both AML and acute lymphoid leukemia (ALL) cases. In AML, they occur more frequently (5–30%) in the subtypes with monocytic components, such as M4, M5a and M5b, based on the French–American–British classification (Schoch *et al.*, 2003; De Braekeleer *et al.*, 2005). Consistent with this, *in vivo* studies in mice have revealed that *MLL*-fusion genes caused AML, which was arrested at the late myelomonocytic stage, regardless of the developmental level of the initiating cells (Cozzio *et al.*, 2003). AML with *MLL*-fusion genes has been reported to have poorer prognosis with combination chemotherapy and stem cell transplantation (the median overall survival: 8.9 months) (Schoch *et al.*, 2003). Therefore, the development of novel therapies against AML with *MLL*-fusion genes should be investigated.

CCAAT/enhancer binding proteins (C/EBPs) are a family of transcription factors that have an important function in the regulation of cellular proliferation and differentiation. In the hematopoietic system, C/EBPα and C/EBPε are required for granulocytic commitment of multipotent myeloid progenitors and terminal differentiation of granulocytes, respectively (Yamanaka *et al.*, 1997; Zhang *et al.*, 2004). The expression and function of C/EBPα and C/EBPε are often altered in AML leukemogenesis. Mutations in *CEBPA* are found in about 10% of AML cases (Pabst *et al.*, 2001a; Gombart *et al.*, 2002). The expression of C/EBPα in

AML cells is inhibited by AML1-ETO or internal tandem duplication of *fms*-like tyrosine kinase 3 (FLT3-ITD), and the ectopic expression of C/EBPα induces granulocytic differentiation in the leukemic cells with these mutated genes (Pabst *et al*., 2001b; Zheng *et al*., 2004). PML-RARα in acute promyelocytic leukemia (APL) inhibits the expression of C/EBPε, and the ectopic expression of either C/EBPα or C/EBPε induces granulocytic differentiation *in vivo* (Truong *et al*., 2003). These studies suggest that the altered expression and function of C/EBPα and C/EBPε are involved in subsets of AML, and that the induction of C/EBPα and C/EBPε can thus induce the differentiation of leukemic cells.

Retinoic acid (RA) is known to induce terminal differentiation of normal myeloid progenitors, and is widely used to induce the differentiation of leukemic cells in APL patients. The application of the differentiation activity of RA to myelomonocytic cells with *MLL*-fusion genes has also been explored (Hemmi and Breitman, 1985; Iijima *et al*., 2004). However, the previous studies did not clarify the importance of the C/EBPs function in their RA-induced monocytic differentiation. This study demonstrated that the growth arrest and monocytic differentiation of myelomonocytic cells with *MLL*-fusion gene is induced by ectopic expression of either C/EBPα or C/EBPε alone, as well as by RA. These findings may lead to a novel therapeutic approach in AML with *MLL*-fusion genes by enhancing C/EBPs functions.

Results

RA inhibited the proliferation and induced the differentiation of myelomonocytic cells with MLL-fusion genes

To see the potential commitment of cell lineage in myelomonocytic cells with *MLL*-fusion genes, human myelomonocytic cell lines with *MLL-AF9*, THP-1 and MOLM-14 cells, were treated with RA. HF-6 cells, a murine cell line established by the introduction of *MLL-SEPT6* derived from t(X;11)(q24;q23) into murine hematopoietic cells were also used (Ono *et al*., 2005). HF-6 cells were assumed to be arrested at the myelomonocytic stage, based on their pale cytoplasm occasionally accompanied by a few vacuoles and azurophilic granules, weakly-positive for myelomonocytic markers Mac-1, Gr-1 and c-Kit, and negative reactions for Sca-1 and CD34. When all of these cell lines were treated with all-*trans* RA (ATRA) or 9-*cis* RA, their proliferation was suppressed in a dose-dependent manner (Figure 1a). HF-6 and THP-1 cells completely died within 7 days after 10^{-6} M of RA (either ATRA or 9-*cis* RA) treatment. However, the inhibitory effect of RA on the proliferation of MOLM-14 cells was partial. The cells gradually increased in number, and repeated exposure to fresh media with 10^{-6} M of RA completely inhibited their growth (data not shown). Morphologically, monocytic differentiation was observed in all the cell lines following RA treatment (10^{-6} M) (Figure 1b). HF-6 cells differentiated by RA were positive for α-naphthyl butyrate staining, which was specific for the monocytic lineage (Figure 1c), and negative for naphthol AS-D chloracetate and myeloperoxidase stainings, which were specific for the myeloid lineage (data not shown). The expression of the monocytic differentiation markers CD11b and CD36 were upregulated with RA treatment in THP-1 and MOLM-14 cells (Figure 1d).

The effects of ATRA or 9-*cis* RA treatment on primary AML cells harboring *MLL*-fusion were also analysed. Three cases of primary AML cells were sorted out according to their surface markers before clonogenic assay (Supplementary Table 1). Small colony-forming units or clusters from leukemic cells (L-CFU as the abbreviation including both of them) were observed on days 11–14. L-CFU was classified in the following three types, granulocyte/macrophage-L-CFU (L-CFU-GM), granulocyte-L-CFU (L-CFU-G) and macrophage-L-CFU (L-CFU-M), according to the cellular contents (Figure 2a). ATRA or 9-*cis* RA induced L-CFU-M formation, mainly small monocytic clusters, in place of L-CFU-GM and L-CFU-G (Figure 2b). An immunophenotypic analysis of L-CFU was performed in case 1, and uncovered the decrease of total cellular number and the increase of CD36-positive cells (Figure 2c). Taken together, these findings suggest that ATRA and 9-*cis* RA treatment inhibited the proliferation of AML cells with *MLL*-fusion genes, accompanied by monocytic differentiation.

C/EBPs were upregulated in RA-induced monocytic differentiation of myelomonocytic cells with MLL-fusion genes

To gain insight into the molecular mechanisms of RA-induced growth arrest and monocytic differentiation of myelomonocytic cells with *MLL*-fusion genes, the expression of C/EBPs was analysed. HF-6 cells weakly expressed the N-terminally truncated (30 kDa isoform: p30) isoforms of C/EBPα, and lesser extent, the functional isoform (42 kDa isoform: p42) of C/EBPα, and did not express C/EBPε. RA upregulated C/EBPα; 9-*cis* RA induced them more than ATRA, and 10^{-6} M was more effective, when compared with 10^{-8} M. The p42 isoform of C/EBPα was upregulated more intensely than the p30 isoform, which was reported to antagonize the p42 isoform (Pabst *et al*., 2001a) (Figure 3a). RA also upregulated the p32 and p30 isoforms of C/EBPε, and lesser extent, the p27 isoform (Figure 3b). The upregulation of *Cebpa* and *Cebpe* mRNAs in HF-6 cells by 10^{-6} M RA was detected in an analysis using quantitative reverse transcription (RT)–PCR (Figure 3c). The induction of the p42 isoform of C/EBPα and the p32 isoform of C/EBPε by RA was also observed in THP-1 and MOLM-14 cells (Figures 3d and e) (Lee *et al*., 2002). However, the induction of the p30 isoform of C/EBPα, and the p30 and p27 isoforms of C/EBPε were not apparent in either of these two cell lines.

Although only two kinds of *MLL*-fusion genes were examined, the findings indicated that myelomonocytic cells with *MLL*-fusion genes were committed to the

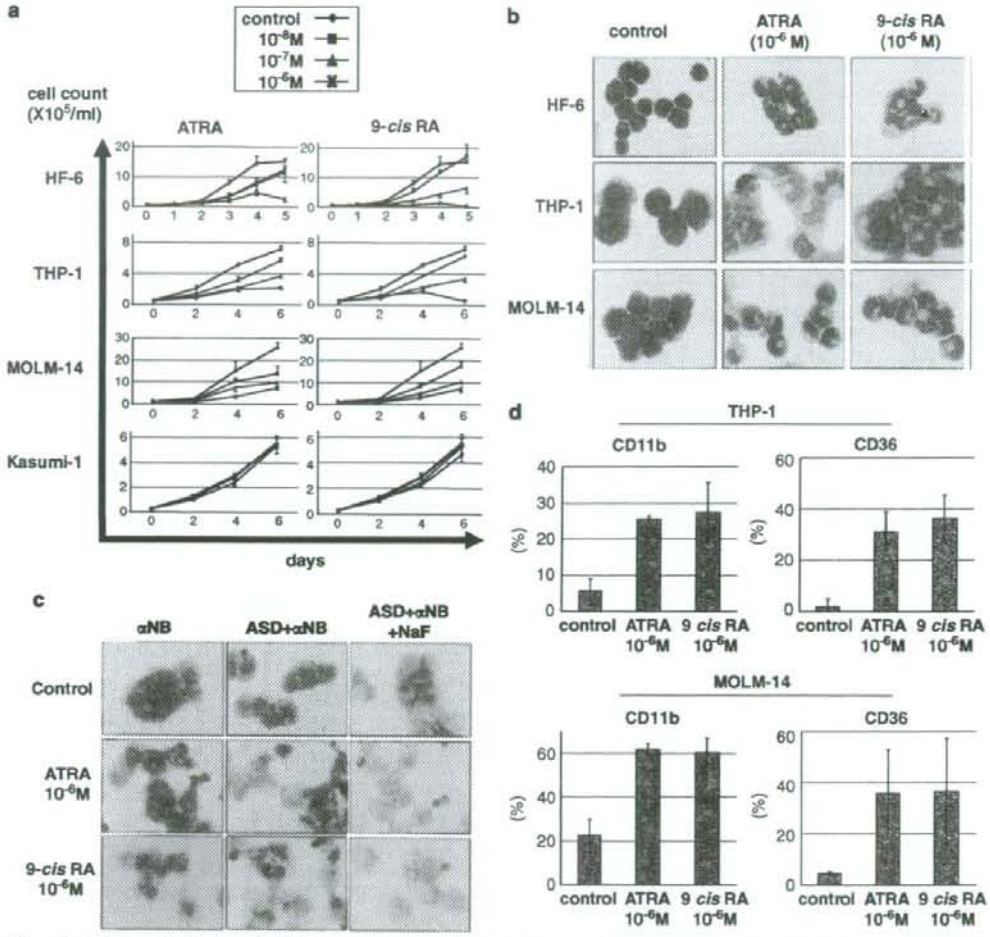

Figure 1 Effects of retinoic acid (RA) on myelomonocytic cells with *MLL*-fusion genes. (**a**) RA-induced growth inhibition of myelomonocytic cells with *MLL*-fusion genes. Kasumi-1 cells were used as a negative control. (**b**) RA-induced monocytic differentiation of myelomonocytic cells with *MLL*-fusion genes. HF-6 cells were cultured with RA for 2 days, and THP-1 and MOLM-14 cells for 5 days. All these cells exhibited an extended, less basophilic cytoplasm with few granules and an irregular shaped-nucleus with indentation after RA treatment. A number of vacuoles were also recognized in RA-treated HF-6 cells. May–Giemsa staining. (**c**) α-naphthyl butyrate (α-NB) staining and inhibition with sodium fluoride (NaF) in HF-6 cells treated with RA. Magnification: ×400 in (**b**) and (**c**). (**d**) The induction of CD11b and CD36 in THP-1 and MOLM-14 cells by 5-day treatment with 10^{-6} M RA. The analyses were performed using flow cytometry.

monocytic lineage and differentiated by RA treatment, with the concomitant upregulation of C/EBPs.

Induction of C/EBPs activity inhibited the cellular growth and promoted the monocytic differentiation in HF-6 cells

To investigate whether the induction of C/EBPs activity could promote the monocytic differentiation and maturation in myelomonocytic cells with *MLL*-fusion genes, inducible forms of C/EBPα or C/EBPε were retrovirally introduced into HF-6 cells. Because C/EBPα and C/EBPε were fused to the estrogen receptor (C/EBPα-ER and C/EBPε-ER, respectively), 4-Hydroxytamoxifen (4-HT) could induce C/EBPs activity (Fukuchi *et al*., 2006; Nakajima *et al*., 2006). Their ectopic expression in HF-6 cells was confirmed by immunoblotting (Figure 4a). HF-6 cells with empty vector (HF-6/pMY) proliferated, but the cellular growth was completely inhibited by the expression of C/EBPα-ER or C/EBPε-ER (Figure 4b). HF-6/pMY cells had morphologically blastic features, whereas HF-6/C/EBPα-ER and HF-6/C/EBPε-ER cells showed monocytic differentiation after 1 day with or without 4-HT stimulation as they did with RA treatment

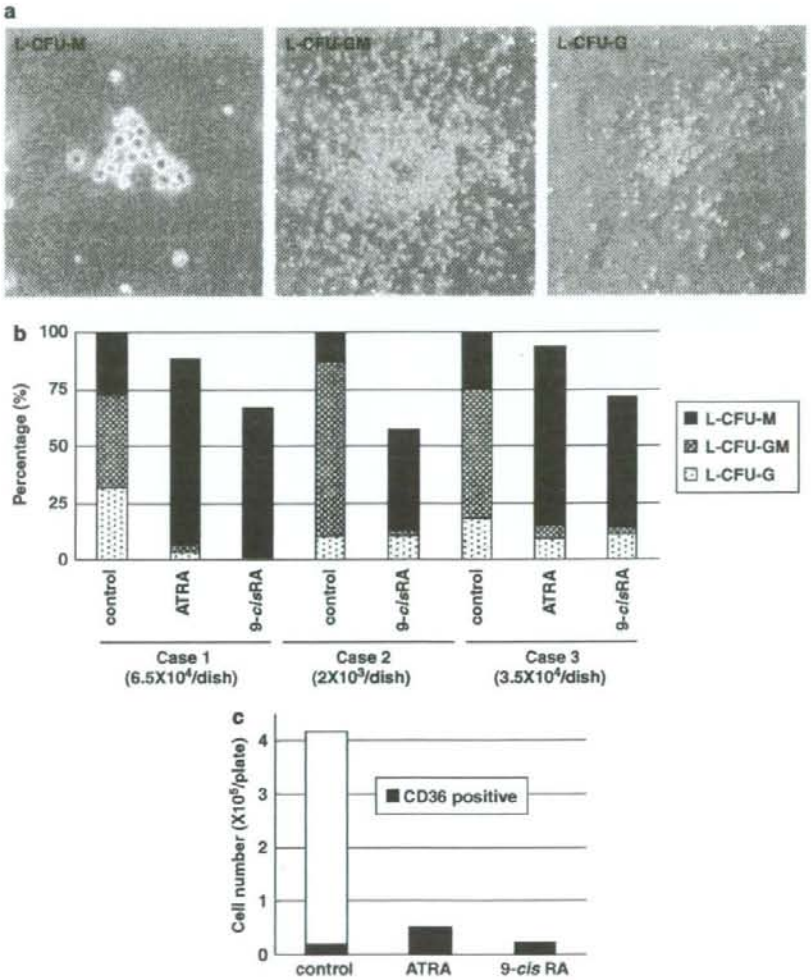

Figure 2 Retinoic acid (RA) inhibited the colony formation and induced monocytic differentiation of primary acute myeloid leukemia (AML) cells with *MLL*-fusion genes. Primary AML cells with *MLL*-fusion genes were sorted out before clonogenic assay, according to the expression of their surface markers (Supplementary Table 1). Colony-formation units from AML samples (L-CFU) with or without 10^{-6} M of all-*trans* RA (ATRA) or 9-*cis* RA were analysed on days 11–14 in triplicate, except for case 2 (one plate per group). (**a**) Representative pictures of macrophage-L-CFU (L-CFU-M), granulocyte/macrophage-L-CFU (L-CFU-GM) and granulocyte-L-CFU (L-CFU-G). Magnification: × 100 (L-CFU-M), × 40 (L-CFU-GM and L-CFU-G) (**b**) ATRA- and 9-*cis* RA-induced monocytic differentiation of primary AML cells with *MLL*-fusion genes. The results of the average number of total L-CFU without RA treatment are shown as 100% in each case. Note that the percentage of L-CFU-M markedly increased after treatment with ATRA or 9-*cis* RA, whereas those of L-CFU-GM and L-CFU-G decreased. (**c**) RA inhibited the proliferation of AML-derived cells and induced CD36-positive cells in case 1. All the cells in the plates for clonogenic assay were collected and counted. Their expression of CD36 was analysed by flow cytometry, and the absolute number of CD36-positive cells was calculated.

(Figure 4c). To quantify the monocytic differentiation of HF-6 cells by inducing C/EBPs activity, the cells were counted by classifying them into three forms; an immature form is monoblastic cells with a basophilic cytoplasm and a round nucleus composed of fine chromatin formation. A mature form is similar to mature macrophages, which has an extended, clear cytoplasm with vacuolation and an indented or lobulated nucleus with coarse chromatin formation. An intermediate form has morphological features between those of an immature and mature form: a basophilic cytoplasm and an indented nucleus with rather fine chromatin formation. The mature forms were not induced in HF-6/pMY cells, but were induced in HF-6/C/EBPα-ER and HF-6/C/EBPε-ER cells, regardless of 4-HT treatment (Figure 4d). Analysis by

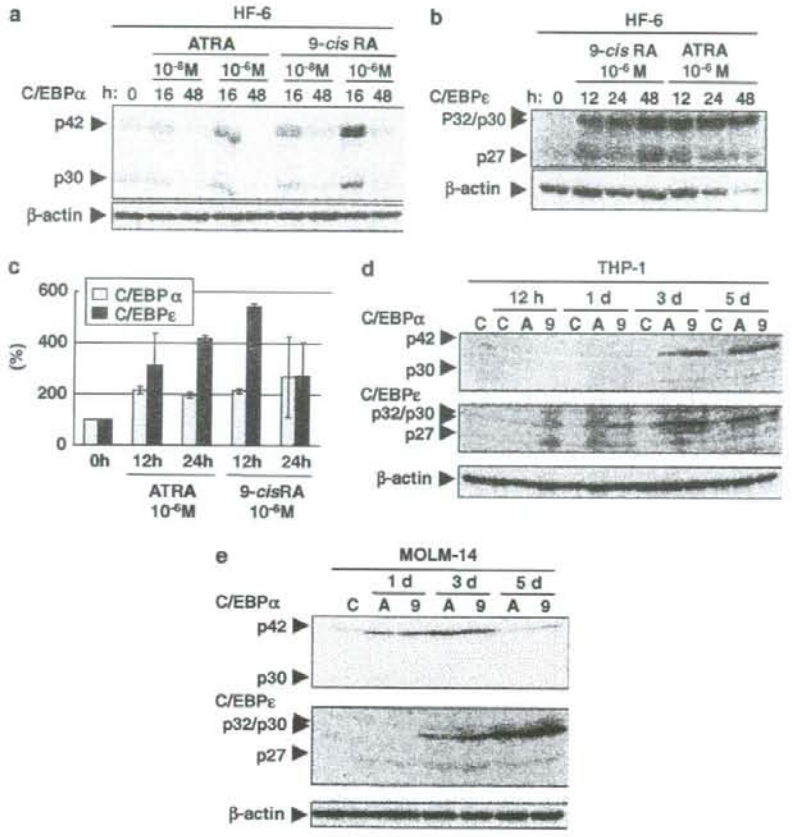

Figure 3 Retinoic acid (RA) induced the expression of CCAAT/enhancer binding proteins (C/EBPs) in myelomonocytic cells with *MLL*-fusion genes. Immunoblotting revealed the induction of (**a**) the p42 isoform of C/EBPα, and (**b**) p32 and p30 isoforms of C/EBPε in HF-6 cells with RA. (**c**) Quantitative reverse transcription (RT)–PCR also revealed the upregulation of C/EBPα and C/EBPε mRNAs in HF-6 cells with RA (10^{-6} M). The mRNA content was measured relative to that of murine *Gapdh*. The relative ratios in regard to the data before RA treatment (at 0 h) are presented in percentages. Upregulation of the p42 isoform of C/EBPα and p32/p30 isoform of C/EBPε by RA was also recognized in (**d**) THP-1 and (**e**) MOLM-14 cells using immunoblotting. C: control, A: treatment with 10^{-6} M of ATRA, 9: treatment with 10^{-6} M of 9-*cis* RA, d: days.

flow cytometry showed marked induction of Mac-1 and Gr-1 in HF-6/C/EBPα-ER and HF-6/C/EBPε-ER cells on day 2 (Figure 4e). Their intensities were higher in the cells expressing C/EBPα-ER than C/EBPε-ER, and enhanced with 4-HT treatment (data not shown). Because the empty vector did not lead to any changes in HF-6 cells as mentioned above, the growth inhibition and monocytic differentiation were thought to be specific for the expression of C/EBPα-ER or C/EBPε-ER.

To evaluate the contribution of apoptosis in growth inhibition of HF-6 cells by induction of C/EBPs activity, the percentage of annexin V-positive/propidium iodide-negative cells was determined in HF-6/C/EBPα-ER or HF-6/C/EBPε-ER cells cultured with 4-HT. After 18 h-incubation with 1 μM of 4-HT, this cell fraction was not increased in HF-6/pMY cells (6.59%), but was induced by C/EBPα or C/EBPε activation in HF-6 cells (44.81 and 26.46%, respectively, Figure 4f).

Taken together, these findings suggested that the induction of either C/EBPα or C/EBPε activity by itself could induce the monocytic differentiation and apoptosis in HF-6 cells.

Changes of mRNA expression in HF-6 cells induced by C/EBPs activation

To observe the expression of the genes associated with cellular proliferation and differentiation in HF-6/C/EBPα-ER or HF-6/C/EBPε-ER cells, their expression levels were determined using quantitative RT–PCR (Figure 5).

We found that the ectopic expression of either C/EBPα-ER or C/EBPε-ER activity markedly decreased *Myc* expression (21 ± 3 and 13 ± 3%, at 12-h incubation with 4-HT, respectively) and upregulated *Sfpi1*, the murine homolog of *PU.1* (454 ± 151 and 345 ± 134% at 4-h incubation with 4-HT, respectively). Although